DYNAMIC BEHAVIOUR OF A CRACKED SHAFT ON ELASTIC SUPPORTS

LIQIANG LIU

Dynamic Behaviour Of A Cracked Shaft On Elastic Supports

by

© Liqiang Liu, B. Eng., M. Eng.

A thesis submitted to the School of Graduate Studies
in partial fulfillment of the requirements
for the degree of Master of Engineering

Faculty of Engineering and Applied Science
Memorial University of Newfoundland

June 1995

St. John's Newfoundland Canada

ISBN 0-612-06130-2

To
My parents Jinkai Liu and Yulan Jia
and
My wife Miao

Abstract

This is a simple but comprehensive study of the dynamic behavior of a shaft with a crack on elastic supports. The analysis is restricted to the single span shaft with uniform circular cross-section. The natural frequency and modes of vibration of a shaft having a transverse crack are investigated using the finite element method. The local flexibility due to the crack is evaluated using the theory of fracture mechanics. The effect of crack depth on the natural behavior is discussed. The results show that an increase in the depth of the of crack magnifies the response amplitude and decreases the natural frequencies. The effect of elastic supports on the dynamic behavior of the shaft is presented through computation. The range of maximum effect is given.

The element stiffness matrix of a cracked shaft considering the longitudinal translation and axial rotation is first presented. This makes it possible to analysize the dynamic response of a practical shaft by FEM. A Fortran-77 program is developed which can be used to calculate the two and three dimensional vibration of a shaft containing more than one transverse crack, concentrated mass and elastic foundation. It can also be used in multi-span shaft with different cross-section and applied to some loads.

Acknowledgements

In my pursuit of the Master degree in Engineering, I have received valuable advice and assistance from a number of people, this is very much appreciated. In particular, I would like to thank:

(a) Dr. M. R. Haddara, my supervisor, for his guidance and support throughout the program, and for his advice and elucidation of the various problems associated with this study.

(b) Dr. J. J. Sharp, Dr. A. S. J. Swamidas and Dr. G. Sabin for their courses and help. Mrs. Moya Crocker for her help during the course of my study.

(c) The School of Graduate Studies for providing funding and teaching assistantships.

(d) Mr. David Press and his staff at the Centre for Computer Aided Engineering for their help in overcoming so many difficulties related to computer work.

(e) Finally, I would like to thank my dear wife, Miao Li, for her patience and understanding.

Contents

Abstract i

Acknowledgements ii

List of Tables vi

List of Figures vii

List of Symbols ix

1 Introduction and Literature Survey 1

1.1 Literature Survey 1

1.2 Objective 4

1.3 Methodology 4

2 Stiffness Matrix Derivation of Space Beam Element with a Crack 5

2.1 Introduction 5

2.2 Crack-Tip Stress Fields for Linear-Elastic Bodies 5

2.2.1 Crack Tip Stress Intensity Factors 5

2.2.2 Evaluation of K_I, K_{II} and K_{III} of The Single Edge Notch 13

2.3 Local Flexibility 21

2.4 Stiffness Matrix of the Cracked Element 29

3 Test of the Program to Solve the Beam Vibration(No Crack) 34

4 The Effect of Elastic Supports and Propeller Inertia on the Dynamic Behaviour 38

4.1 K_1=K_2 40

4.2 $K_1 \neq K_2$ 44

4.3 Effect of The Propeller Inertia 48

4.4 Discussion of The Results 49

5 The Effect of A Crack on the Dynamic Behaviour 51

5.1 Calculation Results 51

5.2 Conclusions 61

6 Stiffness Matrix Derivation of Space Beam Element with a Crack Considering the Axis Translation and Rotation 62

6.1 Local Flexibility 62

6.2 Stiffness Matrix of the Cracked Element 63

7 Conclusions 68

7.1 Conclusions 68

7.2 Recommendations 69

References 70

Appendices 73

A Free Vibration of a Beam **74**

A.1 Bending Vibration Equation of a Beam Subjected to an Axial Force 74

B Mass and Stiffness Matrices Derivation of Space Beam Element **78**

C Flow Chart of Program **85**

D Computer Program in Fortran-77 **88**

List of Tables

3.1 Comparison of Natural Frequencies 37

4.1 First Three Frequencies 40

4.2 First Three Frequencies 44

5.1 First Three Frequencies Corresponding to Different Crack Depth . 53

List of Figures

2.1 The Basic Modes of Crack Surface Displacements. 7

2.2 Coordinates Measured from the Leading Edge of a Crack and the Stress Components in the Crack Tip Stress Field 9

2.3 The Single Edge Notch Test Specimen Under Tension Load 14

2.4 The Single Edge Notch Test Specimen Under Bending Load . . . 16

2.5 The Single Edge Notch Test Specimen Under Shear and Torsion Load 18

2.6 The Single Edge Notch Test Specimen Under Torsion Load 20

2.7 (a) A cracked shaft element in general loading; (b) the crack section of the shaft. 22

2.8 Dimensionless compliances versus crack depth. (a) $\bar{c}_{11}$, $\bar{c}_{15}$, $\bar{c}_{55}$; (b) $\bar{c}_{14}$, $\bar{c}_{44}$, $\bar{c}_{45}$; (c) $\bar{c}_{26}$, $\bar{c}_{36}$, $\bar{c}_{66}$; (d) $\bar{c}_{22}$, $\bar{c}_{33}$. 28

2.9 Simply supported shaft with a cracked element 31

3.1 Flow Chart of the Program 35

3.2 (a) Simple supported; (b) Free; (c) Fixed; (d) Cantilever; (e) Propped 36

4.1 (a) shaft; (b) Mesh of elements 39

4.2 the curve between first frequency and K 41

4.3 the curve between second frequency and K 42

4.4 the curve between third frequency and K 43

4.5 the curve between first frequency and K 45

4.6 the curve between second frequency and K 46

4.7 the curve between third frequency and K 47

4.8 Diagram of a tailed shaft 49

5.1 (a) shaft with a crack; (b) Mesh of elements 52

5.2 Variations of first frequency with different crack depth 54

5.3 Variations of second frequency with different crack depth 55

5.4 Variations of third frequency with different crack depth 56

5.5 Variations of normalized change in first frequency with crack depth 57

5.6 Variations of normalized change in second frequency with crack depth 58

5.7 Variations of normalized change in third frequency with crack depth 59

5.8 First Mode Shape of Shaft with Different Crack Depth 60

6.1 Shaft with Cracked Element 64

A.1 (a) a beam in bending; (b) free body diagram of an element . . . 75

B.1 Space frame member: (a) local directions; (b) global directions. . 79

B.2 Beam element with 8 degrees of freedom 83

List of Symbols

x,y,z	Coordinates in global system
x', y', z'	Coordinates in local system
t	time
M(x,t)	Bending moment of the shaft
V(x,t)	Shear force of the shaft
f(x,t)	External force per unit length of a shaft
A(x)	area of cross-section of a shaft
ρ	Mass density
P	External load
θ	Angle between axial and horizontal directions
E	Young's elasticity modulus
G	Shear modulus of elasticity
ν	Possion ratio
I	Inertia moment of cross-section of shaft
D	Diameter of shaft
R	Radius of shaft
J	Polar moment of inertia of shaft per unit length
$\sigma_x, \sigma_y, \sigma_z$	Tension stress
$\tau_{xy}, \tau_{yz}, \tau_{zx}$	Shear stress
a	Depth of a crack

h,b	the gemetric size of a sample
K_I, K_{II}, K_{III}	Three kinds of stress intensity factors
u_i	displacement of crack tip
$\bar{c}_{ij}$	Dimensionless compliance
C_{loc}	Local flexibility matrix
K_1, K_2	Stiffness of elastic supports
J(a)	J-integral
$[K]$	Stiffness matrix
$[M]$	Mass matrix

Chapter 1

Introduction and Literature Survey

A propeller shaft is an important part of ship propulsion. Shaft vibration monitoring has been receiving increasing attention in recent years. The failures of shafts due to fatigue cracks makes it imperative to have an accurate estimation of shaft natural vibration characteristics in the design stage. Vibration monitoring has the greatest potential in crack detection since it can be carried out without dismantling any part of the machine and be done usually even under operating condition.

1.1 Literature Survey

Fatigue cracking in a shaft is one of the main causes of catastrophic failure which is described by Jack and Patterson (1976). Since a crack changes the stiffness that influences the dynamic behavior of the shaft , vibration monitoring could be used as a means of detecting crack initiation and growth. Kolzow (1974) first pointed out that the vibration monitoring could be useful in detecting crack initiation and growth. Therefore a detailed study of the vibrational behavior of shaft with transverse cracks is necessary.

Since the middle 1970s, many researchers have realized the importance of this problem. The first work done by Dimarogonas (1970) and Pafelias (1974) introduced the bending stiffness description of a rotor crack which is determined from compliance measurements. The incorporation of the stiffness change caused by a crack into the equation of motion was dealt with in the literature by Dimarogonas (1976).

Gasch (1976, 1993) developed a hinge model for Laval rotors (massless shaft), in which he replaced the crack mechanism by an additional crack flexibility and switched it on and off according to whether the crack was closed or open. He discovered that resonances would occur as the rotation reached $\frac{1}{2}$, $\frac{1}{3}$, etc., of the shaft bending frequencies.

Henry and Okah-Avae (1976) employed the equations of motion with a shaft section interia unequal to that of the cracked shaft, and concluded that there would be resonances due to the crack when the rotational speed equal to $\frac{1}{n}$ of the first critical speed where n is an odd integer. They also found that the vibration response due to the crack was hardly detectable when the rotational speed exceeded the first critical speed.

Mayes and Davies (1976) Mayes (1977) performed a detailed analytical and experimental investigation of turbine shafts with cracks. They derived a rough analytical estimation of the crack compliance based on the energy principle. Although they considered the nonlinear equation for a simple rotor, they obtained analytical solutions by considering an open crack which led to a shaft with dissimilar moments of inertia in two perpendicular directions.

Grabowski and Mahrenholtz (1982; 1980) argued that in a shaft of practical interest the shaft deflection due to its own weight is orders of magnitude greater than the vibration amplitude. Therefore he suggests that non-linearity does not affect the shaft response since the crack opens and closes regularly with the rotation.

Using the concept that a transverse crack in a structural member introduces local flexibility due to the strain energy concentration in the vicinity of the crack tip under load, Dimorogonas and Papadopoulos (1983), Dimorogonas and Paipetis (1983) and Papadopoulos and Dimarogonas (1987) derived the complete local flexibility matrix of a cracked, rotating shaft and verified it experimentally. They observed the local flexibility of the shaft due to the crack and developed an analytical expression for the crack local flexibility in relation to the crack depth. They also showed the influence of the crack on the dynamic response of the rotor.

Ziebarth and Baumgartner(1981) established their crack model on the basis of detailed (but quasistatic) experimental investigation. They consequently formulated the equations of motion in stationary coordinates and applied them to practical turbine rotors. Then they compared the analytical results with the results of model test. As practical crack indicators, they suggested significant peaks in vibration amplitudes, shifting of natural frequencies, unstable vibrations, and changes in the double-frequency vibration component.

Dirr and Schmalhorsts (1987) described the crack more accurately than others by a 3-dimensional finite element analysis and successfully simulated the vibrations of a cracked test rotor on the basis of measured crack shapes.

Qian et al (1990) derived the element stiffness matrix of a beam with a crack from an integration of the stress intensity factors and then established a finite element mode (FEM) of a cracked beam.

Most of the investigators concentrated on the stiffness changes due to a crack, and these researchers only considered the case that the crack is perpendicular to the axis of shaft.

1.2 Objective

In this study, a finite element model is employed to analyze the dynamic behaviour of a shaft having a crack and supported on elastic bearings. Through the investigation, some relationships between natural frequencies of shaft and crack depth and stiffness of elastic supports should be found. This work will also provide some useful results for experimental investigation in the next stage.

1.3 Methodology

In this study, the first step is to give a theoretically description of the free vibration of a beam. Furthermore, a finite element model is formulated to analyze the effect of elastic supports on the dynamic behaviour of a non-crack shaft and give an approximate evaluation of propeller effect.

In order to derive the stiffness matrix of cracked element, a fracture mechanics approach is used to study the effect of the presence of a crack on the dynamic characteristics of the shaft.

At last, a Fortran-77 computer program was developed.

Chapter 2

Stiffness Matrix Derivation of Space Beam Element with a Crack

2.1 Introduction

The element stiffness matrix of a beam with a crack was derived from an integration of the stress intensity factors and then a finite element model(FEM) of a cracked beam was established by Qian et al(1990). Sekhar and Prabhu (1992) also presented a similar approach .

2.2 Crack-Tip Stress Fields for Linear-Elastic Bodies

2.2.1 Crack Tip Stress Intensity Factors

Fracture studies of structural elements have been revolutionized in the recent twenty years by the analysis of their sensitivity to flaws or cracklike defects. Within these studies an essential ingredient is reasonable and proper stress analysis including especially the flaw with its high local elevations of stresses from which fracture progresses through various crack propagation mechanisms(stress corrosion, fatigue,etc.).

Full studies of fracture behavior cover both the stress analysis aspects and the material behavior in terms of resistance to the stresses imposed. The redistribution of stress in a body due to the introduction of a crack or notch may be begun by methods of linear-elastic stress analysis. Of course the greatest attention should be paid to the high level of stresses at or surrounding the crack tip which will usually be accompanied by at least some plasticity and other non-linear effects. Nevertheless linear-elastic stress analysis properly forms the basis of most current fracture analysis for at least "small scale yielding" where all substantial non-linearity is confined within a linear-elastic field surrounding the crack tip. Consequently, the character and significant parameters of linear-elastic crack tip fields will be given first attention.

The surface of a crack has the dominating influence on the distribution of stresses near and around the crack tip. Other remote boundaries and loading forces affect only the intensity of the local stress field at the tip.

The stress fields near crack tips can be divided into three basic types, each associated with a local mode of deformation as illustrated in Figure 2.1.(Tada et al, 1973)

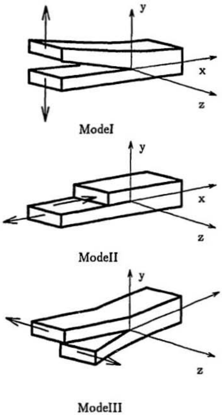

Figure 2.1: The Basic Modes of Crack Surface Displacements.

Mode I is the opening mode which is associated with local displacement in which the crack surfaces move directly apart (symmetric with respect to the x-y and x-z planes). Mode II is the edge-sliding mode, which is characterized by displacements in which the crack surfaces slide over one another perpendicular to the leading edge of the crack (symmetric with respect to the x-y plane and skew-symmetric with respect to the x-z plane). Mode III is tearing mode, finds the crack surface sliding with respect to one another parallel to the leading edge (skew-symmetric with respect to the x-y plane and x-z plane). The superposition of these three modes is sufficient to describe the most general 3-dimensional case of local crack-tip deformation and stress fields.(Tada et al,1973)

The most direct approach to determination of the stress and displacement fields associated with each mode follows in the manner of Irwin (1957), based on the method of Westergaard (1939). Modes I and II can be analyzed as 2-dimensional plane-extensional problems of the theory of elasticity which are subdivided as symmetric and skew-symmetric, respectively, with respect to the crack plane. Mode III can be regarded as the 2-dimensional pure shear (or torsion) problem. Referring to Figure 2.2 for notation, the resulting stress and displacement fields are given below:

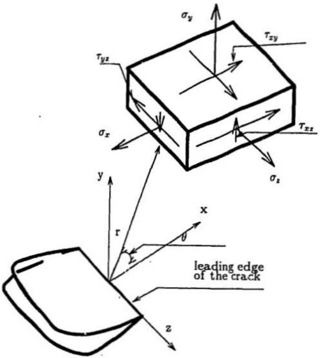

Figure 2.2: Coordinates Measured from the Leading Edge of a Crack and the Stress Components in the Crack Tip Stress Field

Mode I

For plane stress

$$\sigma_x = \frac{K_I}{(2\pi r)^{\frac{1}{2}}} cos\frac{\theta}{2}[1 - sin\frac{\theta}{2}sin\frac{3\theta}{2}] + \sigma_{x0} + O(r^{\frac{1}{2}}) \tag{2.1}$$

$$\sigma_y = \frac{K_I}{(2\pi r)^{\frac{1}{2}}} cos\frac{\theta}{2}[1 + sin\frac{\theta}{2}sin\frac{3\theta}{2}] + O(r^{\frac{1}{2}}) \tag{2.2}$$

$$\tau_{xy} = \frac{K_I}{(2\pi r)^{\frac{1}{2}}} cos\frac{\theta}{2}sin\frac{\theta}{2}cos\frac{3\theta}{2} + O(r^{\frac{1}{2}}) \tag{2.3}$$

and for plane strain (with higher order terms omitted)

$$\sigma_z = \nu(\sigma_x + \sigma_y) \tag{2.4}$$

$$\tau_{xz} = 0 \tag{2.5}$$

$$\tau_{yz} = 0 \tag{2.6}$$

$$u = \frac{K_I}{G}[\frac{r}{(2\pi)}]^{\frac{1}{2}} cos\frac{\theta}{2}[1 - 2\nu + sin^2\frac{\theta}{2}] \tag{2.7}$$

$$v = \frac{K_I}{G}[\frac{r}{(2\pi)}]^{\frac{1}{2}} sin\frac{\theta}{2}[2 - 2\nu - cos^2\frac{\theta}{2}] \tag{2.8}$$

$$w = 0 \tag{2.9}$$

Mode II

For plane stress

$$\sigma_x = -\frac{K_{II}}{(2\pi r)^{\frac{1}{2}}} sin\frac{\theta}{2}[2 + cos\frac{\theta}{2} cos\frac{3\theta}{2}] + \sigma_{x0} + O(r^{\frac{1}{2}}) \tag{2.10}$$

$$\sigma_y = \frac{K_{II}}{(2\pi r)^{\frac{1}{2}}} sin\frac{\theta}{2} cos\frac{\theta}{2} cos\frac{3\theta}{2} + O(r^{\frac{1}{2}}) \tag{2.11}$$

$$\tau_{xy} = \frac{K_{II}}{(2\pi r)^{\frac{1}{2}}} cos\frac{\theta}{2}[1 - sin\frac{\theta}{2} sin\frac{3\theta}{2}] + O(r^{\frac{1}{2}}) \tag{2.12}$$

and for plane strain (with higher order terms omitted)

$$\sigma_z = \nu(\sigma_x + \sigma_y) \tag{2.13}$$

$$\tau_{xz} = 0 \tag{2.14}$$

$$\tau_{yz} = 0 \tag{2.15}$$

$$u = \frac{K_{II}}{G}[\frac{r}{(2\pi)}]^{\frac{1}{2}} sin\frac{\theta}{2}[2 - 2\nu + cos^2\frac{\theta}{2}] \tag{2.16}$$

$$v = \frac{K_{II}}{G}[\frac{r}{(2\pi)}]^{\frac{1}{2}} cos\frac{\theta}{2}[-1 + 2\nu + sin^2\frac{\theta}{2}] \tag{2.17}$$

$$w = 0 \tag{2.18}$$

Mode III

For plane stress

$$\tau_{xz} = -\frac{K_{III}}{(2\pi r)^{\frac{1}{2}}} sin\frac{\theta}{2} + \tau_{xz_0} + O(r^{\frac{1}{2}}) \tag{2.19}$$

$$\tau_{yz} = \frac{K_{III}}{(2\pi r)^{\frac{1}{2}}} cos\frac{\theta}{2} + O(r^{\frac{1}{2}}) \tag{2.20}$$

$$\sigma_x = 0 \tag{2.21}$$

$$\sigma_y = 0 \tag{2.22}$$

$$\sigma_z = 0 \tag{2.23}$$

$$\tau_{xy} = 0 \tag{2.24}$$

$$u = 0 \tag{2.25}$$

$$v = 0 \tag{2.26}$$

$$w = \frac{K_{III}}{G}[\frac{2r}{\pi}]^{\frac{1}{2}} sin\frac{\theta}{2} \tag{2.27}$$

Equations for Mode I and Mode II have been written for the case of plane strain (that is ,w=0) but can be changed to plane stress easily by taking $\sigma_z = 0$ and replacing Poisson's ratio, ν, in the displacements with an appropriate value, $\frac{\nu}{(1+\nu)}$.

In equations for modes I, II and III, higher order terms such as uniform stresses parallel to the crack, σ_{x0} and τ_{xz_0}, and terms of the order of square root of r, $O(r^{\frac{1}{2}})$, are as indicated. However, normally these terms are omitted since as r becomes small compared to planar dimensions (in the x-y plane) these higher order terms become negligible compared to the leading $\frac{1}{\sqrt{r}}$ term. Therefore these leading terms are the linear-elastic crack tip stress (and displacement) fields.

The parameters K_I, K_{II} and K_{III} in these equations are called crack tip stress (field) intensity factors for the corresponding three modes. Since K_I, K_{II} and K_{III} are not functions of the coordinates, r and θ, they represent the strength of the stress fields surrounding the crack tip. Alternately they may be mathematically viewed as the strengths of the $\frac{1}{\sqrt{r}}$ stress singularities at the crack tip. Their values are determined by other boundaries of the body and the loads imposed, consequently formulas for their evaluation come from a complete stress analysis of a given configuration and loading.

2.2.2 Evaluation of K_I, K_{II} and K_{III} of The Single Edge Notch

From H. Tada, et al (1973), K_I, K_{II} and K_{III} can be evaluated for the single edge notch specimen by following formulas:

1. K_I

The loading condition and size are shown in Figure 2.3

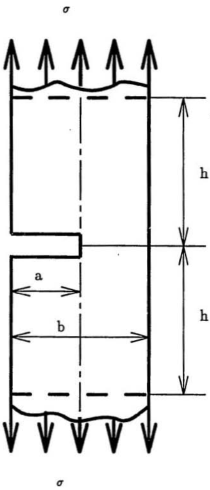

Figure 2.3: The Single Edge Notch Test Specimen Under Tension Load

$$K_I = \sigma\sqrt{\pi a}F(\frac{a}{b}) \tag{2.28}$$

The numerical values of $F(\frac{a}{b})$ can be calculated by following empirical Formulas.

$$F(\frac{a}{b}) = 1.12 - 0.231(\frac{a}{b}) + 10.55(\frac{a}{b})^2 - 21.72(\frac{a}{b})^3 + 30.39(\frac{a}{b})^4 \tag{2.29}$$

The accuracy is 0.5% for $\frac{a}{b}$ less than 0.6.

$$F(\frac{a}{b}) = 0.265(1 - \frac{a}{b})^4 + \frac{0.857 + 0.265\frac{a}{b}}{(1 - \frac{a}{b})^{\frac{3}{2}}} \tag{2.30}$$

The accuracy is better than 1% for $\frac{a}{b}$ less than 0.2 and 0.5% for $\frac{a}{b}$ greater than or equal 0.2.

$$F(\frac{a}{b}) = \sqrt{\frac{2b}{\pi a} tan \frac{\pi a}{2b}} \frac{(0.752 + 2.02(\frac{a}{b}) + 0.37(1 - sin\frac{\pi a}{2b})^3}{cos\frac{\pi a}{2b}} \tag{2.31}$$

The accuracy is better than 0.5% for any $\frac{a}{b}$

For the loading condition shown in Figure 2.4

$$K_I = \sigma\sqrt{\pi a}F(\frac{a}{b}) \tag{2.32}$$

Numerical values of $F(\frac{a}{b})$ can be obtained by following empirical formulas.

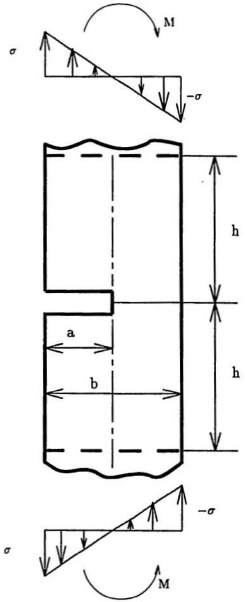

Figure 2.4: The Single Edge Notch Test Specimen Under Bending Load

$$F(\frac{a}{b}) = 1.122 - 1.40\frac{a}{b} + 7.33(\frac{a}{b})^2 - 13.08(\frac{a}{b})^3 + 14.0(\frac{a}{b})^4 \qquad (2.33)$$

The accuracy is 0.2% for $\frac{a}{b}$ less than or equal 0.6.

$$F(\frac{a}{b}) = \sqrt{\frac{2b}{\pi a} tan \frac{\pi a}{2b}} \frac{(0.923 + 0.199(1 - sin\frac{\pi a}{2b})^4}{cos\frac{\pi a}{2b}} \qquad (2.34)$$

The accuracy is better than 0.5% for any $\frac{a}{b}$

2. K_{II} and K_{III}

For loading condition shown in Figure 2.5

$$K_{II} = Q\frac{2}{\sqrt{\pi a}} F_{II}(\frac{a}{b}) \qquad (2.35)$$

$$K_{III} = T\frac{2}{\sqrt{\pi a}} F_{III}(\frac{a}{b}) \qquad (2.36)$$

$$F_{II}(\frac{a}{b}) = \frac{1.3 - 0.65(\frac{a}{b}) + 0.37(\frac{a}{b})^2 + 0.28(\frac{a}{b})^3}{\sqrt{1 - \frac{a}{b}}} \qquad (2.37)$$

$$F_{III}(\frac{a}{b}) = \sqrt{\frac{\frac{\pi a}{b}}{sin\frac{\pi a}{b}}} \qquad (2.38)$$

The accuracy of F_{II} is better than 1% for any $\frac{a}{b}$

F_{III} is exact.

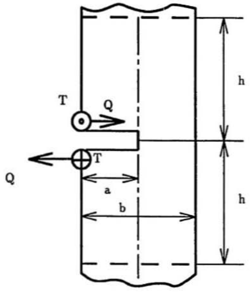

Figure 2.5: The Single Edge Notch Test Specimen Under Shear and Torsion Load

For loading condition shown in Figure 2.6

$$K_{II} = \tau\sqrt{\pi a}F_{II}(\frac{a}{b}) \tag{2.39}$$

$$K_{III} = \tau_l\sqrt{\pi a}F_{III}(\frac{a}{b}) \tag{2.40}$$

$$F_{II}(\frac{a}{b}) = \frac{1.122 - 0.56(\frac{a}{b}) + 0.085(\frac{a}{b})^2 + 0.18(\frac{a}{b})^3}{\sqrt{1-\frac{a}{b}}} \tag{2.41}$$

$$F_{III}(\frac{a}{b}) = \sqrt{\frac{2b}{\pi a}tan\frac{\pi a}{2b}} \tag{2.42}$$

The accuracy of F_{II} is better than 2% for any $\frac{a}{b}$

F_{III} is exact.

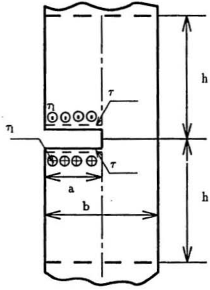

Figure 2.6: The Single Edge Notch Test Specimen Under Torsion Load

2.3 Local Flexibility

Consider a shaft with given stiffness properties, radius R=D/2, where D is the diameter of the shaft, and a transverse crack of depth a ,shown in Figure 2.7(a) and (b). The shaft is loaded with axial force P_1, shear forces P_2 and P_3, bending moments P_4 and P_5 and torsional moment P_6. The dimension of the local flexibility matrix depends on the number of degree of freedom, here it is 6 $\times$ 6.

H. Tada's equation (Tada et al, 1973) gives the additional displacement u_i due to a crack of depth a, in the i direction, as

$$u_i = \frac{\partial}{\partial P_i} \int_0^a J(a)da \tag{2.43}$$

where J(a) is the Strain Energy Density Function (SEDF) and P_i is the corresponding load. The SEDF is (Dimarogonas and Paipetis ,1983)

$$J = \frac{1}{E'}[(\sum_{i=1}^{6} K_{Ii})^2 + (\sum_{i=1}^{6} K_{IIi})^2 + m(\sum_{i=1}^{6} K_{IIIi})^2] \tag{2.44}$$

Where $E' = E$ or $E/(1-\nu^2)$ for plane stress and plane strain respectively, E is the modulus of elasticity, $m = 1+\nu$, ν is the Poisson ratio (ν =0.3 for steel) and K_{ij} are the Crack Stress Intensity Factors (SIF) for the i = I, II, III modes and for j =1,2,...,6, the load index.

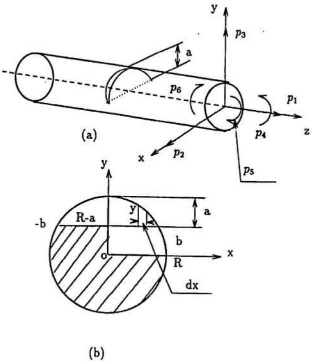

Figure 2.7: (a) A cracked shaft element in general loading; (b) the crack section of the shaft.

The local flexibility due to the crack per unit width is, by definition (Dimarogonas and Paipetis, 1983)

$$c_{ij} = \frac{\partial u_i}{\partial P_j} \tag{2.45}$$

That is

$$c_{ij} = \frac{\partial^2}{\partial P_i \partial P_j}[\int_A J(A)dA] \tag{2.46}$$

or, after integrating along the width 2b of the crack,

$$c_{ij} = \frac{\partial^2}{\partial P_i \partial P_j}[\int_{-b}^{b}\int_0^a J(a)dadx] \tag{2.47}$$

The value of SIF in equation(2.44) are well known from the literature (Tada et al, 1973) for a strip of unit thickness with a transverse crack. Since the energy density is a scalar, it is permissible to integrate along the tip of the crack it being assumed that the crack depth is variable and that the stress intensity factor is given for the elementary strip. It is known that this approximation yields acceptable results for engineering accuracy (Dimarogonas and Paipetis, 1983) . From reference (Tada et al, 1973)

$$K_{I1} = \sigma_1 \sqrt{\pi \alpha} F_1(\frac{\alpha}{h}) \tag{2.48}$$

$$\sigma_1 = \frac{P_1}{\pi R^2} \tag{2.49}$$

$$K_{I4} = \sigma_4 \sqrt{\pi \alpha} F_1(\frac{\alpha}{h}) \tag{2.50}$$

$$\sigma_4 = \frac{4P_4}{\pi R^4} \tag{2.51}$$

$$K_{I5} = \sigma_5\sqrt{\pi\alpha}F_2(\frac{\alpha}{h}) \tag{2.52}$$

$$\sigma_5 = \frac{4P_5}{\pi R^4}(R^2 - x^2)^{\frac{1}{2}} \tag{2.53}$$

$$K_{I2} = K_{I3} = K_{I6} = 0$$

$$K_{II3} = \sigma_3\sqrt{\pi\alpha}F_{II}(\frac{\alpha}{h}) \tag{2.54}$$

$$\sigma_3 = \frac{kP_3}{\pi R^2} \tag{2.55}$$

$$K_{II6} = \sigma_{6II}\sqrt{\pi\alpha}F_{II}(\frac{\alpha}{h}) \tag{2.56}$$

$$\sigma_{6II} = \frac{2P_6 x}{\pi R^4} \tag{2.57}$$

$$K_{II1} = K_{II2} = K_{II4} = K_{II5} = 0$$

$$K_{III2} = \sigma_2\sqrt{\pi\alpha}F_{III}(\frac{\alpha}{h}) \tag{2.58}$$

$$\sigma_2 = \frac{kP_2}{\pi R^2} \tag{2.59}$$

$$K_{III6} = \sigma_{6III}\sqrt{\pi\alpha}F_{III}(\frac{\alpha}{h}) \tag{2.60}$$

$$\sigma_{6III} = \frac{2P_6(R^2 - x^2)^{\frac{1}{2}}}{\pi R^4} \tag{2.61}$$

$$K_{III1} = K_{III3} = K_{III4} = K_{III5} = 0$$

where

$$F_1(\frac{\alpha}{h}) = (\frac{tan\lambda}{\lambda})^{\frac{1}{2}}[0.752 + 2.02(\frac{\alpha}{h}) + 0.37(1 - sin\lambda)^3]/cos\lambda \tag{2.62}$$

$$F_2(\frac{\alpha}{h}) = (\frac{tan\lambda}{\lambda})^{\frac{1}{2}}[0.923 + 0.199(1 - sin\lambda)^4]/cos\lambda \tag{2.63}$$

$$F_{II}(\frac{\alpha}{h}) = [1.122 - 0.561(\frac{\alpha}{h}) + 0.085(\frac{\alpha^2}{h}) + 0.18(\frac{\alpha}{h})^3]/(1 - \frac{\alpha}{h})^{\frac{1}{2}} \tag{2.64}$$

$$F_{III}(\frac{\alpha}{h}) = (\frac{tan\lambda}{\lambda})^{\frac{1}{2}} \tag{2.65}$$

$$\lambda = \frac{\pi\alpha}{2h}$$

Here $k = 6(1+\nu)/(7+6\nu)$ is a shape coefficient for circular cross section.

Combining relations (2.44), (2.47) and (2.48)-(2.65) yields the dimensionless terms of the compliance matrix:

$$\bar{c_{11}} = \frac{\pi ER}{1-\nu^2}c_{11} = 4\int_0^{\bar{a}}\int_0^{\bar{b}} \bar{x}F_1^2(\bar{h})d\bar{x}d\bar{y} \tag{2.66}$$

$$\tag{2.67}$$

$$\bar{c_{15}} = \frac{\pi ER^2}{1-\nu^2}c_{15} = 16\int_0^{\bar{a}}\int_0^{\bar{b}} \bar{y}(1-\bar{x}^2)^{\frac{1}{2}}F_1(\bar{h})F_2(\bar{h})d\bar{x}d\bar{y} \tag{2.68}$$

$$\tag{2.69}$$

$$\bar{c_{55}} = \frac{\pi E R^3}{1-\nu^2} c_{55} = 64 \int_0^{\bar{a}} \int_0^{\bar{b}} \bar{y}(1-\bar{x}^2) F_2^2(\bar{h}) d\bar{x} d\bar{y} \tag{2.70}$$

(2.71)

$$\bar{c_{44}} = \frac{\pi E R^3}{1-\nu^2} c_{44} = 32 \int_0^{\bar{a}} \int_0^{\bar{b}} \bar{x}^2 \bar{y} F_1^2(\bar{h}) d\bar{x} d\bar{y} \tag{2.72}$$

(2.73)

$$\bar{c_{14}} = \frac{\pi E R^2}{1-\nu^2} c_{14} = 8 \int_0^{\bar{a}} \int_0^{\bar{b}} \bar{x}\bar{y} F_1^2(\bar{h}) d\bar{x} d\bar{y} \tag{2.74}$$

(2.75)

$$\bar{c_{45}} = \frac{\pi E R^3}{1-\nu^2} c_{45} = 64 \int_0^{\bar{a}} \int_0^{\bar{b}} \bar{x}\bar{y}\sqrt{1-\bar{x}^2} F_1(\bar{h}) F_2(\bar{h}) d\bar{x} d\bar{y} \tag{2.76}$$

(2.77)

$$\bar{c_{33}} = \frac{\pi E R}{1-\nu^2} c_{33} = 4 \int_0^{\bar{a}} \int_0^{\bar{b}} \bar{x} F_{II}^2(\bar{h}) d\bar{x} d\bar{y} \tag{2.78}$$

(2.79)

$$\bar{c_{22}} = \frac{\pi E R}{1-\nu^2} c_{22} = 4 \int_0^{\bar{a}} \int_0^{\bar{b}} \bar{y} F_{III}^2(\bar{h}) d\bar{x} d\bar{y} \tag{2.80}$$

(2.81)

$$\bar{c_{62}} = \frac{\pi E R^2}{1-\nu^2} c_{62} = 8 \int_0^{\bar{a}} \int_0^{\bar{b}} \sqrt{1-\bar{x}^2}\bar{y} F_{III}^2(\bar{h}) d\bar{x} d\bar{y} \tag{2.82}$$

$$\tag{2.83}$$

$$\bar{c_{63}} = \frac{\pi E R^2}{1-\nu^2} c_{63} = 8 \int_0^{\bar{a}} \int_0^{\bar{b}} \bar{x}\bar{y} F_{II}^2(\bar{h}) d\bar{x} d\bar{y} \tag{2.84}$$

$$\tag{2.85}$$

$$\bar{c_{66}} = \frac{\pi E R^3}{1-\nu^2} c_{66} = 16 \int_0^{\bar{a}} \int_0^{\bar{b}} [A_1 + m A_2] d\bar{x} d\bar{y} \tag{2.86}$$

$$\tag{2.87}$$

Where $A_1 = \bar{x}^2\bar{y}F_{II}^2(\bar{h})$,$A_2 = (1-\bar{x}^2)\bar{y}F_{III}^2(\bar{h})$ and $\bar{x} = x/R$,$\bar{y} = y/R$, $\bar{h} = y/h$,$\bar{b} = b/R$.

The dimensionless compliance matrix is then.

$$\bar{c} = \begin{bmatrix} \bar{c}_{11} & 0 & 0 & \bar{c}_{14} & \bar{c}_{15} & 0 \\ 0 & \bar{c}_{22} & 0 & 0 & 0 & \bar{c}_{26} \\ 0 & 0 & \bar{c}_{33} & 0 & 0 & \bar{c}_{36} \\ \bar{c}_{41} & 0 & 0 & \bar{c}_{44} & \bar{c}_{45} & 0 \\ \bar{c}_{51} & 0 & 0 & \bar{c}_{54} & \bar{c}_{55} & 0 \\ 0 & \bar{c}_{62} & \bar{c}_{63} & 0 & 0 & \bar{c}_{66} \end{bmatrix} \tag{2.88}$$

The elements of this matrix are computed and plotted in Figure 2.8.

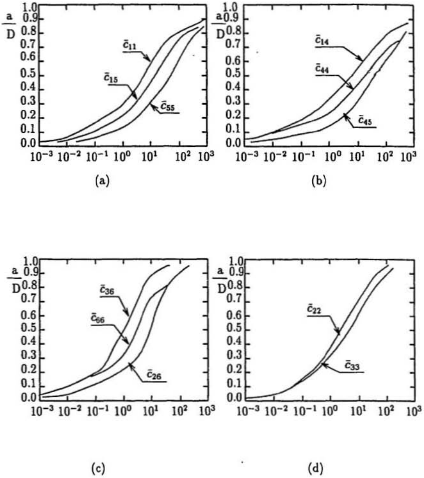

Figure 2.8: Dimensionless compliances versus crack depth. (a) $\bar{c}_{11}$, $\bar{c}_{15}$, $\bar{c}_{55}$; (b) $\bar{c}_{14}$, $\bar{c}_{44}$, $\bar{c}_{45}$; (c) $\bar{c}_{26}$, $\bar{c}_{36}$, $\bar{c}_{66}$; (d) $\bar{c}_{22}$, $\bar{c}_{33}$.

Then the local flexibility matrix due to the crack equations (2.66)-(2.87) and equation (2.88) yields

$$C_{loc} = \frac{1}{F_0}\begin{bmatrix} \bar{c}_{11}R & 0 & 0 & \bar{c}_{14} & \bar{c}_{15} & 0 \\ 0 & \bar{c}_{22}R & 0 & 0 & 0 & \bar{c}_{26} \\ 0 & 0 & \bar{c}_{33}R & 0 & 0 & \bar{c}_{36} \\ \bar{c}_{41} & 0 & 0 & \bar{c}_{44}/R & \bar{c}_{45}/R & 0 \\ \bar{c}_{51} & 0 & 0 & \bar{c}_{54}/R & \bar{c}_{55}/R & 0 \\ 0 & \bar{c}_{62} & \bar{c}_{63} & 0 & 0 & \bar{c}_{66}/R \end{bmatrix} \tag{2.89}$$

where $\bar{c_{ij}}$ $(i,j = 1,2,...,6)$ are the dimensionless compliance coefficients and $F_0 = \pi E R^2/(1-\nu^2)$.

When neglecting the axial translation and rotation, the local flexibility matrix becomes

$$C_{loc} = \frac{1}{F_0}\begin{bmatrix} \bar{c}_{22}R & 0 & 0 & 0 \\ 0 & \bar{c}_{33}R & 0 & 0 \\ 0 & 0 & \bar{c}_{44}/R & \bar{c}_{45}/R \\ 0 & 0 & \bar{c}_{54}/R & \bar{c}_{55}/R \end{bmatrix} \tag{2.90}$$

2.4 Stiffness Matrix of the Cracked Element

According to the principle of Saint-Venant, the stress field is affected only in the region adjacent to the crack. Therefore, the element stiffness matrix, except for the cracked element, may be regarded as unchanged under a certain limitation of element size (Qian et al, 1990) . The additional stress energy of a crack has been studied thoroughly in fracture mechanics and the flexibility coefficient, expressed by a stress intensity factor, can be easily derived by means of Castigliano's theorem in the linear-elastic range.

Considering a shaft divided into elements as shown in Figure 2.9 . The behavior of the elements situated to the right of the cracked element may be regarded as external forces applied to the cracked element, while the behaviour of elements situated to its left may be regarded as constraints (Qian et al,1990; Sekhar and Prabhu, 1992). Thus, the flexibility matrix of a cracked element with constraints may be calculated.

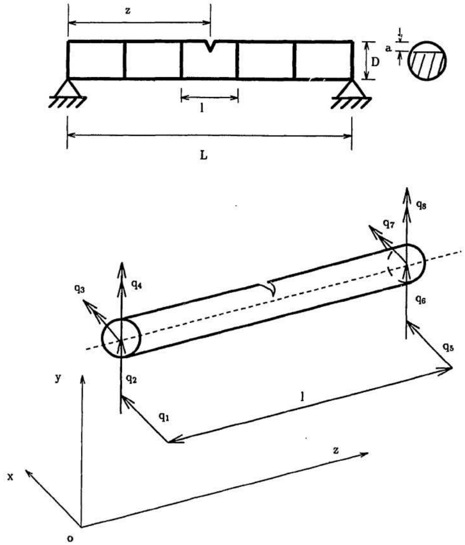

Figure 2.9: Simply supported shaft with a cracked element

With the shearing action neglected, and by using the strain energy, the flexibility coefficients for an element without a crack (see Figure 2.9) can be derived in the form

$$C_0 = \frac{l}{6EI} \begin{bmatrix} 2l^2 & 0 & 0 & 3l \\ 0 & 2l^2 & -3l & 0 \\ 0 & -3l & 6 & 0 \\ 3l & 0 & 0 & 6 \end{bmatrix} \tag{2.91}$$

Here EI is the bending stiffness and l is the element length.

The additional flexibility matrix due to the crack is shcwn in equation(2.90)

The total flexibility matrix for the cracked element is given as

$$[C] = [C_0] + [C_{loc}] \tag{2.92}$$

From the equilibrium conditions (Figure 2.9)

$$q_1 = -q_5$$

$$q_2 = -q_6$$

$$q_3 = -q_7 + lq_6$$

$$q_4 = -lq_5 - q_8$$

$$q_5 = q_5$$

$$q_6 = q_6$$

$$q_7 = q_7$$

$$q_8 = q_8$$

That is

$$(q_1, q_2, ..., q_8)^T = [T](q_5, q_6, q_7, q_8)^T \tag{2.93}$$

where the transformation matrix [T] is

$$[T] = \begin{bmatrix} -1 & 0 & 0 & 0 \\ 0 & -1 & 0 & 0 \\ 0 & l & -1 & 0 \\ -l & 0 & 0 & -1 \\ 1 & 0 & 0 & 0 \\ 0 & 1 & 0 & 0 \\ 0 & 0 & 1 & 0 \\ 0 & 0 & 0 & 1 \end{bmatrix}$$

So the stiffness matrix of the cracked element can be written as

$$[K_c] = [T][C]^{-1}[T]^T \tag{2.94}$$

Chapter 3

Test of the Program to Solve the Beam Vibration(No Crack)

According to the model described in Appendix A , a FORTRAN-77 program is written. The program flow chart is shown in Figure 3.1. To check the program, a comparison with the analytical solution for beams having different boundary conditions (Weaver and Johnston ,1987) is made. The comparison is shown in Table 3.1.

Five cases are considered. These are simple support, free, fixed, cantilever and propped beams which are shown in Figure 3.2. The beam is divided into four elements, each of which has the same properties E,I,ρ and A.

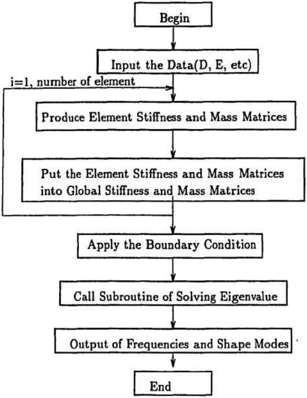

Figure 3.1: Flow Chart of the Program

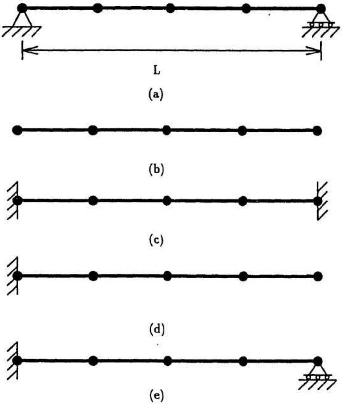

Figure 3.2: (a) Simple supported; (b) Free; (c) Fixed; (d) Cantilever; (e) Propped

Table 3.1: Comparison of Natural Frequencies

Structure	Mode	Exact Solution	Solution of the Program
Simple	1	2.560 E6	2.563 E6
	2	4.100 E7	4.130 E7
	3	2.050 E8	2.150 E8
Free	1	1.316 E7	1.318 E7
	2	9.999 E7	1.013 E8
	3	3.843 E8	3.843 E8
Fixed	1	1.316 E7	1.311 E7
	2	9.999 E7	1.018 E8
	3	3.843 E8	4.009 E8
Cantilever	1	3.250 E5	3.256 E5
	2	1.276 E7	1.279 E7
	3	1.001 E8	1.016 E8
Propped	1	6.252 E6	6.258 E6
	2	6.656 E7	6.646 E7
	3	2.855 E8	2.986 E8

From the Table, it is found that there is a very good agreement between analytical solution and calculated results.

Chapter 4

The Effect of Elastic Supports and Propeller Inertia on the Dynamic Behaviour

In the dynamic calculation of a propeller shaft, the bearing supports can be considered as elastic supports. The difference of the stiffness of bearings and their distribution may affect the dynamic behaviour of shaft greatly. This is important for the designer to optimize the alignment of the shaft.

Figure 4.1 shows a one span of shaft with elastic supports at two ends. The boundary supports are expressed by two springs in two directions pendicular to each other. In the figure, K_1 and K_2 represent the stiffnesses of the elastic springs at the two ends.

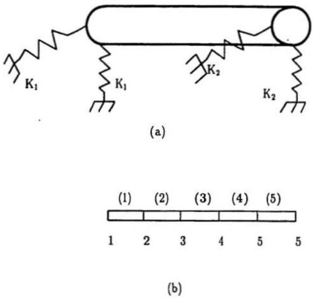

Figure 4.1: (a) shaft; (b) Mesh of elements

Table 4.1: First Three Frequencies

K	w_1	w_2	w_3
rigid	0.6407E6	0.1033E8	0.5375E8
5E12	0.6395E6	0.1027E8	0.5316E8
5E11	0.6329E6	0.9807E8	0.4761E8
5E10	0.5666E6	0.6284E7	0.1926E8
5E09	0.2617E6	0.1138E7	0.5042E7
5E08	0.3869E5	0.1217E6	0.3463E7
5E07	0.4637E4	0.1185E5	0.3314E7

4.1 $K_1 = K_2$

When the stiffnesses of the springs at the two ends of the shaft are the same as K, the different value of the stiffnesses have great effect on the natural behaviour of the shaft. The results are shown in Table 4.1. In the calculation, the shaft is divided into four elements. The value of stiffnesses varies from finite value to a infinite value(rigid). Figure 4.2 - Figure 4.4 show the curves between the value of K and first three natural frequencies w_1, w_2 and w_3.

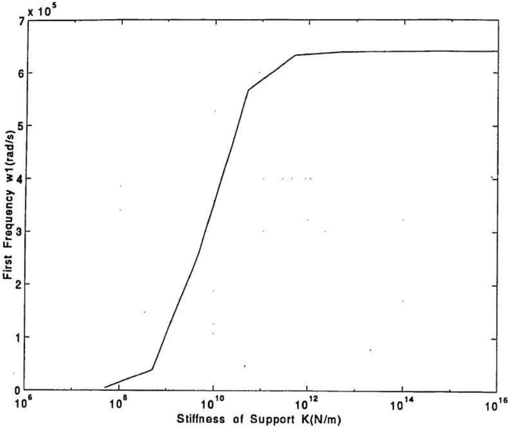

Figure 4.2: the curve between first frequency and K

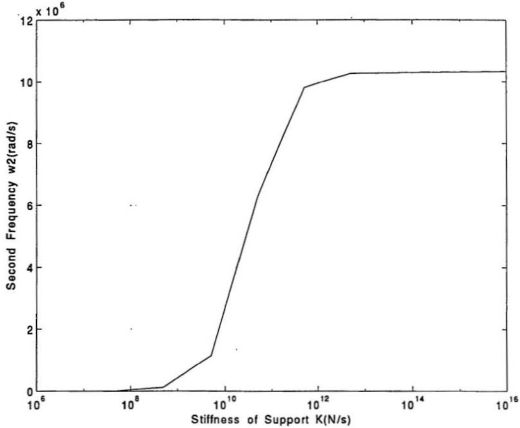

Figure 4.3: the curve between second frequency and K

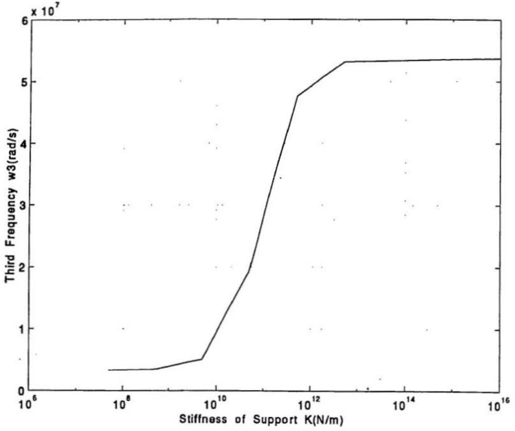

Figure 4.4: the curve between third frequency and K

Table 4.2: First Three Frequencies

K_1/K_2	w_1/w_{01}	w_2/w_{02}	w_3/w_{03}
1	1.000	1.000	1.000
2	1.030	1.1143	1.2113
3	1.040	1.1523	1.2965
4	1.0454	1.1711	1.3390
5	1.0482	1.1822	1.3645
6	1.0508	1.1895	1.3806
10	1.05489	1.2040	1.4123

4.2 $K_1 \neq K_2$

In a practical engineering problem, the bearings at the two ends of the shaft are different. So the effect due to the different values of springs on the natural behaviour should be considered. In this part, I use the value of $\frac{K_1}{K_2}$ to represent the difference between K_1 and K_2. The results are shown in Table 4.2. In the table, w_{01}, w_{02} and w_{03} are the first,second and third frequencies respectively when K_1 equal to K_2. Figure 4.5 –Figure 4.7 show the curves between $\frac{w_1}{w_{01}}$ and $\frac{K_1}{K_2}$, $\frac{w_2}{w_{02}}$ and $\frac{K_1}{K_2}$, and, $\frac{w_3}{w_{03}}$ and $\frac{K_1}{K_2}$.

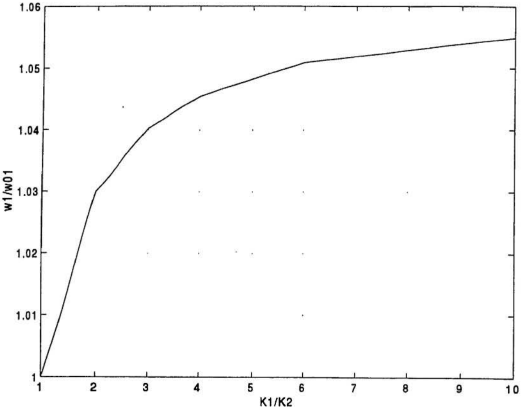

Figure 4.5: the curve between first frequency and K

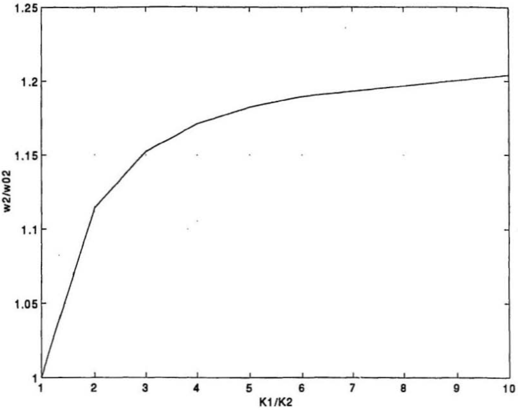

Figure 4.6: the curve between second frequency and K

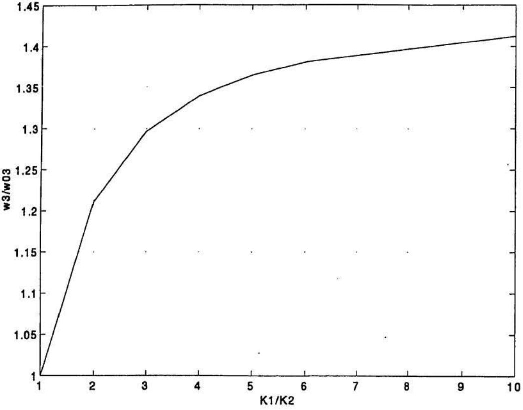

Figure 4.7: the curve between third frequency and K

4.3 Effect of The Propeller Inertia

The effect of propeller inertia will be considered in the boundary conditions to the propeller.

$$EI\frac{\partial^4 w(x,t)}{\partial x^4} + \rho A\frac{\partial^2 w(x,t)}{\partial t^2} = 0 \tag{4.1}$$

For a shaft shown in Figure 4.8, the boundary conditions become

(1) x=0, y=0 and M=0

(2) $x = l_1$, y=0 , $\frac{\partial y_{l_1+}}{\partial x} = \frac{\partial y_{l_1-}}{\partial x}$

and

$\frac{\partial^2 y_{l_1+}}{\partial x^2} = \frac{\partial^2 y_{l_1-}}{\partial x^2}$

(3) x=l

$\frac{\partial^3 y}{\partial x^3} = -\frac{M}{EI}\frac{\partial^2 y}{\partial x^2}$

and

$\frac{\partial^2 y}{\partial x^2} = -\frac{J}{EI}\frac{\partial^3 y}{\partial x \partial t^2}$

Where

J is the mass polar moment of inertia of propeller.

The natural frequencies of following example is carried out.

the lumped mass is 32500kg. and lumped inertia moment is 16300kgm^2. The diameter of shaft is .25m.

The results are:

(1) No lumped mass and inertia moment

w_1=0.1908x10^6(rad/s)

w_2=0.8366x10^6(rad/s)

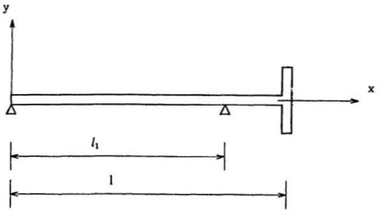

Figure 4.8: Diagram of a tailed shaft

w_1=0.4363x10^7(rad/s)

(2) Only consider the lumped mass

w_1=0.1138x10^4(rad/s)

w_2=0.4923x10^6(rad/s)

w_1=0.3977x10^7(rad/s)

(3) Both lumped mass and inertia moment are considered

w_1=0.6604x10^3(rad/s)

w_2=0.1376x10^5(rad/s)

w_1=0.5202x10^6(rad/s)

4.4 Discussion of The Results

Results of the calculation show that :

A. Results of the calculations shown in Figures 4.2 to 4.4 show that for a certain range of the values of the bearing stiffness, the natural frequencies of the shaft are very sensitive to variations in the bearing stiffness. Within that range the natural frequencies increase rapidly as the stiffness increases. For values of bearing stiffness outside that range the natural frequencies remain almost unchanged as the stiffness changes. When the bearing stiffness is below a certain range, the bearing becomes as a "simple" support, while above that range, the bearing behaves as "fixed" support.

B. When the stiffnesses of elastic supports at the two ends of shaft are not same.

1. With the increase of the value of K_1/K_2, the natural frequencies also increase. However, the effect on lower mode frequencies is less than higher mode frequencies.

2. When the value of K_1/K_2 is larger than a certain number(for example, larger than 6 or 7), with the increase of K_1/K_2, the natural frequencies have very little change.

C. Consideration of the inertia of the propeller decreases the natural frequencies of the system. From the results, it can be found that the frequencies will decrease by considering of lumped mass and inertia moment.

Chapter 5

The Effect of A Crack on the Dynamic Behaviour

5.1 Calculation Results

According to the finite element model described in Chapter 4, a program is written to calculate the natural dynamic behaviour of a cracked shaft.

When the crack is assumed to affect only stiffness, the natural frequencies are obtained by solving the eigenvalue problem $[K] - \omega^2[M]=0$.

Take a one span of beam with a crack at the middle of the beam. The diameter of beam is D, and the depth of crack is a. The mesh of elements are shown in Figure 5.1

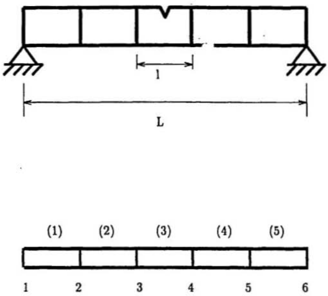

Figure 5.1: (a) shaft with a crack; (b) Mesh of elements

Table 5.1: First Three Frequencies Corresponding to Different Crack Depth

a/D	w_1	w_2	w_3
0.0	0.6406E6	0.1033E8	0.5377E8
0.1	0.6276E6	0.1032E8	0.5371E8
0.2	0.5350E6	0.1029E8	0.5310E8
0.3	0.4156E6	0.9918E7	0.3387E8
0.4	0.2935E6	0.1012E8	0.2813E8
0.5	0.1624E6	0.1000E8	0.2365E8

The results are shown in Table 5.1, Figure 5.2 – Figure 5.7. In the table and figures, w_1, w_2 and w_3 are the first,second and third frequencies respectively, w_{01}, w_{02} and w_{03} are the first,second and third frequencies respectively when the depth of crack is zero, delta w_1, delta w_2 and delta w_3 are w_1-w_{01}, w_2-w_{02} and w_3-w_{03}. The first mode shapes cooresponding to different crack depth are shown in Figure 5.8.

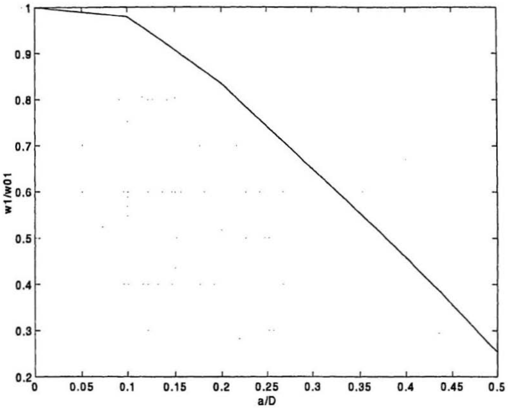

Figure 5.2: Variations of first frequency with different crack depth

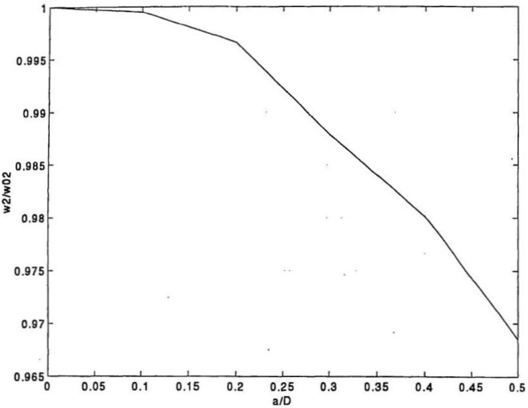

Figure 5.3: Variations of second frequency with different crack depth

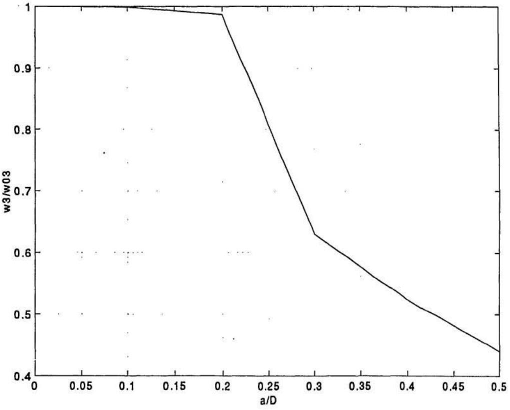

Figure 5.4: Variations of third frequency with different crack depth

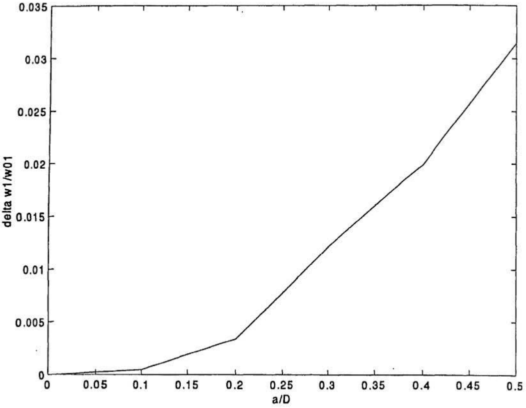

Figure 5.5: Variations of normalized change in first frequency with crack depth

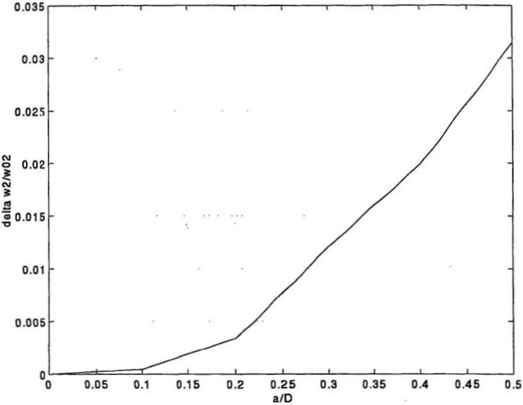

Figure 5.6: Variations of normalized change in second frequency with crack depth

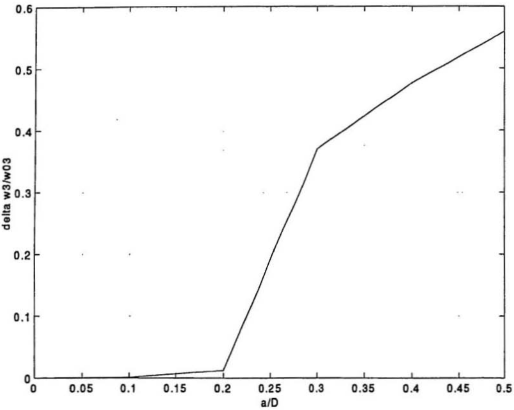

Figure 5.7: Variations of normalized change in third frequency with crack depth

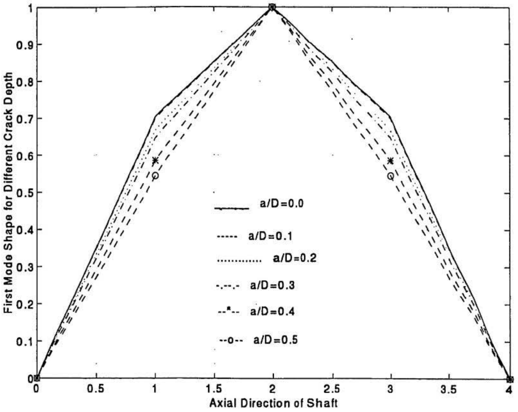

Figure 5.8: First Mode Shape of Shaft with Different Crack Depth

5.2 Conclusions

From the results, we can get conclusions as follows:

1. As expected, the natural frequencies decrease when the crack occurs, and the maximum amplitudes of the mode shapes become larger.

2. As the crack depth becomes larger, the amplitudes of the mode shapes become larger, and the values of natural frequencies become smaller. The general trend of the decrease in natural frequencies with the increase in crack depth is also observed at higher frequencies.

3. When the crack occurs close to the middle of the shaft, the maximum amplitude of the mode shape occurs.

Chapter 6

Stiffness Matrix Derivation of Space Beam Element with a Crack Considering the Axis Translation and Rotation

In practical engineering, the shaft is rotating under the normal operation at some rotation speed. Therefore it is necessary to study the the crack effect on the shaft torsional vibration. Figure 2.7 depicts a typical cracked shaft in general loading.

6.1 Local Flexibility

Consider a shaft with given stiffness properties, radius R=D/2, where D is the diameter of the shaft, and a transverse crack of depth a ,shown in Figure 2.7(a) and (b). The shaft is loaded with axial force P_1,shear forces P_2 and P_3, Bending moment P_4 and P_5 and torsional moment P_6. The dimension of the local flexibility matrix depends on the number of degrees of freedom, here 6 $\times$ 6.

From Chapter 2, the dimensionless local compliance matrix is then.

$$\bar{c} = \begin{bmatrix} \bar{c}_{11} & 0 & 0 & \bar{c}_{14} & \bar{c}_{15} & 0 \\ 0 & \bar{c}_{22} & 0 & 0 & 0 & \bar{c}_{26} \\ 0 & 0 & \bar{c}_{33} & 0 & 0 & \bar{c}_{36} \\ \bar{c}_{41} & 0 & 0 & \bar{c}_{44} & \bar{c}_{45} & 0 \\ \bar{c}_{51} & 0 & 0 & \bar{c}_{54} & \bar{c}_{55} & 0 \\ 0 & \bar{c}_{62} & \bar{c}_{63} & 0 & 0 & \bar{c}_{66} \end{bmatrix} \tag{6.1}$$

The values of elements of this matrix are computed according to equation (2.66) - (2.87).

Then the local flexibility matrix due to the crack is shown in following equation.

$$C_{loc} = \frac{1}{F_0} \begin{bmatrix} \bar{c}_{11}R & 0 & 0 & \bar{c}_{14} & \bar{c}_{15} & 0 \\ 0 & \bar{c}_{22}R & 0 & 0 & 0 & \bar{c}_{26} \\ 0 & 0 & \bar{c}_{33}R & 0 & 0 & \bar{c}_{36} \\ \bar{c}_{41} & 0 & 0 & \bar{c}_{44}/R & \bar{c}_{45}/R & 0 \\ \bar{c}_{51} & 0 & 0 & \bar{c}_{54}/R & \bar{c}_{55}/R & 0 \\ 0 & \bar{c}_{62} & \bar{c}_{63} & 0 & 0 & \bar{c}_{66}/R \end{bmatrix} \tag{6.2}$$

where $\bar{c}_{ij}$ $(i,j = 1,2,...,6)$ are the dimensionless compliance coefficients and $F_0 = \pi E R^2/(1-\nu^2)$.

6.2 Stiffness Matrix of the Cracked Element

Consider a shaft divided into elements as shown in Figure 6.1 .

With the shearing action neglected, and by using the strain energy, the flexibility coefficients for an element without a crack can be derived in the form

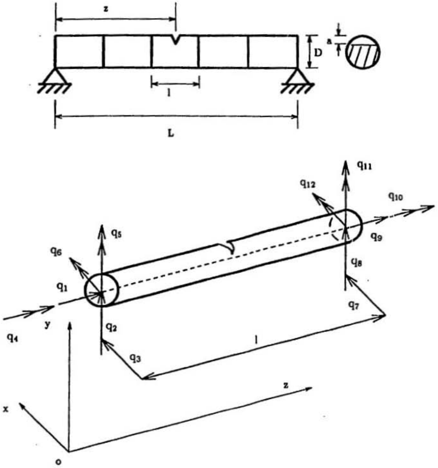

Figure 6.1: Shaft with Cracked Element

$$C_0 = \begin{bmatrix} \frac{l}{EA} & 0 & 0 & 0 & 0 & 0 \\ 0 & \frac{l^3}{3EI} & 0 & 0 & 0 & \frac{l^2}{2EI} \\ 0 & 0 & \frac{l^3}{3EI} & 0 & -\frac{l^2}{2EI} & 0 \\ 0 & 0 & 0 & \frac{l}{JG} & 0 & 0 \\ 0 & 0 & -\frac{l^2}{2EI} & 0 & \frac{l}{EI} & 0 \\ 0 & \frac{l^2}{2EI} & 0 & 0 & 0 & \frac{l}{EI} \end{bmatrix} \tag{6.3}$$

Here EI is the bending stiffness, G is torsional shear modulus, J is torsional inertia moment and l is the element length.

The additional local flexibility matrix due to the crack is shown in equation(6.2).

The total flexibility matrix for the cracked element is given as

$$[C] = [C_0] + [C_{loc}] \tag{6.4}$$

From the equilibrium conditions (Figure 6.1)

$$q_1 = -q_7$$

$$q_2 = -q_8$$

$$q_3 = -q_9$$

$$q_4 = -lq_{10}$$

$$q_5 = lq_9 - q_{11}$$

$$q_6 = -lq_8 - q_{12}$$

$$q_7 = q_7$$

$$q_8 = q_8$$

$$q_9 = q_9$$

$$q_{10} = q_{10}$$

$$q_{11} = q_{11}$$

$$q_{12} = q_{12}$$

That is

$$(q_1, q_2, ..., q_{12})^T = [T](q_7, q_8, ..., q_{12})^T \tag{6.5}$$

where the transformation matrix [T] is

$$[T] = \begin{bmatrix} -1 & 0 & 0 & 0 & 0 & 0 \\ 0 & -1 & 0 & 0 & 0 & 0 \\ 0 & 0 & -1 & 0 & 0 & 0 \\ 0 & 0 & 0 & -1 & 0 & 0 \\ 0 & 0 & l & 0 & -1 & 0 \\ 0 & -l & 0 & 0 & 0 & -1 \\ 1 & 0 & 0 & 0 & 0 & 0 \\ 0 & 1 & 0 & 0 & 0 & 0 \\ 0 & 0 & 1 & 0 & 0 & 0 \\ 0 & 0 & 0 & 1 & 0 & 0 \\ 0 & 0 & 0 & 0 & 1 & 0 \\ 0 & 0 & 0 & 0 & 0 & 1 \end{bmatrix}$$

So the stiffness matrix of the cracked element can be written as

$$[K_c] = [T][C]^{-1}[T]^T \tag{6.6}$$

When without crack

$$[K_c] = [T][C_0]^{-1}[T]^T \tag{6.7}$$

where $[C_0]^{-1}$ is

$$[C_0]^{-1} = \begin{bmatrix} \frac{EA}{l} & 0 & 0 & 0 & 0 & 0 \\ 0 & \frac{12EI}{l^3} & 0 & 0 & 0 & -\frac{6EI}{l^2} \\ 0 & 0 & \frac{12EI}{l^3} & 0 & \frac{6EI}{l^2} & 0 \\ 0 & 0 & 0 & \frac{JG}{l} & 0 & 0 \\ 0 & 0 & \frac{6EI}{l^2} & 0 & \frac{4EI}{l} & 0 \\ 0 & -\frac{6EI}{l^2} & 0 & 0 & 0 & \frac{4EI}{l} \end{bmatrix} \tag{6.8}$$

So the stiffness matrix of element is

$$[K] = [T][C_0]^{-1}[T]^T =$$

$$\begin{bmatrix} \frac{EA}{l} & 0 & 0 & 0 & 0 & 0 & -\frac{EA}{l} & 0 & 0 & 0 & 0 & 0 \\ 0 & \frac{12EI}{l^3} & 0 & 0 & 0 & \frac{6EI}{l^2} & 0 & -\frac{12EI}{l^3} & 0 & 0 & 0 & \frac{6EI}{l^2} \\ 0 & 0 & \frac{12EI}{l^3} & 0 & -\frac{6EI}{l^2} & 0 & 0 & 0 & -\frac{12EI}{l^3} & 0 & -\frac{6EI}{l^2} & 0 \\ 0 & 0 & 0 & \frac{JG}{l} & 0 & 0 & 0 & 0 & 0 & -\frac{JG}{l} & 0 & 0 \\ 0 & 0 & -\frac{6EI}{l^2} & 0 & \frac{4EI}{l} & 0 & 0 & 0 & \frac{6EI}{l^2} & 0 & \frac{2EI}{l} & 0 \\ 0 & \frac{6EI}{l^2} & 0 & 0 & 0 & \frac{4EI}{l} & 0 & -\frac{6EI}{l^2} & 0 & 0 & 0 & \frac{2EI}{l} \\ -\frac{EA}{l} & 0 & 0 & 0 & 0 & 0 & \frac{EA}{l} & 0 & 0 & 0 & 0 & 0 \\ 0 & -\frac{12EI}{l^3} & 0 & 0 & 0 & -\frac{6EI}{l^2} & 0 & \frac{12EI}{l^3} & 0 & 0 & 0 & -\frac{6EI}{l^2} \\ 0 & 0 & -\frac{12EI}{l^3} & 0 & \frac{6EI}{l^2} & 0 & 0 & 0 & \frac{12EI}{l^3} & 0 & \frac{6EI}{l^2} & 0 \\ 0 & 0 & 0 & -\frac{JG}{l} & 0 & 0 & 0 & 0 & 0 & \frac{JG}{l} & 0 & 0 \\ 0 & 0 & -\frac{6EI}{l^2} & 0 & \frac{2EI}{l} & 0 & 0 & 0 & \frac{6EI}{l^2} & 0 & \frac{4EI}{l} & 0 \\ 0 & \frac{6EI}{l^2} & 0 & 0 & 0 & \frac{2EI}{l} & 0 & -\frac{6EI}{l^2} & 0 & 0 & 0 & \frac{4EI}{l} \end{bmatrix} \tag{6.9}$$

This is the general element stiffness matrix of beam without crack.

Chapter 7

Conclusions

7.1 Conclusions

The stiffness of elastic supports of the shaft has great effect on the natural behaviour of the shaft. In the case that the stiffnesses of the elastic supports at the two ends of shaft are the same , (a) with the increase of the stiffness, the natural frequencies also increase; (b) when the stiffness of the elastic supports is larger than a value (which depends on the mode), the natural frequencies are almost constant and approach the natural frequencies when the supports are rigid. (c) for a shaft with similar elastic supports, the natural frequencies vary rapidly when the stiffness is within a certain range. This phenomenon should be considered in alignment of a shaft. When the stiffnesses of elastic supports at the two ends of shaft are not the same. (a) with the increase of stiffness difference between two supports, the natural frequencies also increase; and the effect on lower mode frequencies is less than higher mode frequencies. (b) when the stiffness difference between two supports is big enough, the natural frequencies have very little change.

For a shaft with a crack, the crack effect on the natural behaviour of the shaft is shown in the following aspects.

1, As expected, the natural frequencies decreases when the crack occurs, and the maximum amplitudes of the mode shapes become larger.

2, As the crack depth becomes larger, the amplitudes of the mode shapes become larger, and the values of natural frequencies become smaller. The general trend of the decrease in natural frequencies with the increase in crack depth is also observed at higher frequencies.

3, When the crack occurs close to the middle of the shaft, the maximum amplitude of the mode shape occurs.

In practical engineering, measuring the changes in an adequate number of the natural frequencies can be used to detect the crack. It is important for an engineer to discover the crack as early as possible and prevent damage of the shaft due to the presence of a crack.

7.2 Recommendations

This study carries out the calculation results obtained by finite element method. However, further studies should be done in following topics:

1. Experiments should be done in order to compare with calculation results.

2. In practical shafts, the cracks may occur in any direction, how the crack affect the dynamic characteristics should be studied further.

REFERENCES

Dimarogonas, A. D. , 1970, "Dynamic Response of Cracked Rotors", General Electric Company, Schenectady NY

Dimarogonas, A. D. , 1976, "Vibration Engineering", West Publishers, St. Paul

Dimarogonas, A. D., and Paipetis, S. A. , 1983, "Analytical Methods in Rotor Dynamics", Applied Science Publishers

Dimarogonas, A. D. and Papadopoulos, C. A. , 1983, "Vibration of Cracked Shafts in Bending", J. of Sound and Vibration, 91, pp 583-593.

Dirr, B. O. and Schmalhorsts, B. K. , 1987, "Crack Depth Analysis of a rotating Shaft by Vibration Measurement", Rotating Machinery Dynamics, vol 2, 11th Bienniul Conference on Mechanical Vibration and Noise, Boston, DE vol 2, ASME, pp 607-614

Gasch, R. , 1976, "Dynamic Behavior of a Simple Rotor with a Cross-sectional crack", Vibration in Rotating Machinery, Paper No C178/76, Institution of Mechanical engineers Conference Publication,

Gasch, R. , 1993, "A Survey of the Dynamic Behavior of a Simple Rotating Shaft with a Transverse Crack", J. of Sound and Vibration, 160(2), pp 313-332

Grabowski, B. and Mahrenholtz, O. , 1982, "Theoretical and Experimental Investigations of Shaft Vibrations in Turbomachinery excited by Crack", Proceedings International Conference on Rotordynamic Problems in Power Plants, IFToMM, Rome, pp 507-514

Grabowski, B. , 1980, "The Vibrational Behavior of a Turbine Rotor Containing a Transverse Crack", J. of mechanical Design, 102, pp 140-146

Henry, T. A. and Okah-Avae, B. E. , 1976, "Vibration in Cracked Shafts", in vibrations in rotating Machinery, Institution of mechanical Engineers, London, pp 15-19

Irwin, G. R. , 1957, "Analysis of Stresses and Strains Near the End of a Crack Transversing a Plate", Transactions, ASME, Journal of Applied Mechanics, Vol. 24, pp 361.

Jack, A. R. and Patterson, A. N. , 1976, "Cracking in 500 MW LP Rotor Shafts", 1st Mechanical Engineering Conference.

Kolzow, D. R. , 1974, "Abnormal Vibration–a symptom to cracked rotors" Technical information letter, General Electric Company, TIL-727-4, Apr

Mayes, I. W. , 1977, "Crack Propagation in rotating Shafts", ASME paper 77-DET-164

Mayes, I. W. and Davies, W. G. R. , 1976, "The Vibration Behavior of a Rotating Shaft System Containing a Transverse Crack", in vibrations in rotating Machinery, Institution of mechanical Engineers, London, pp 53-63

Pafelias, T. , 1974, "Dynamic Behavior of a Cracked Rotor" Technical information Series, General Electric Company, No DF-74-LS-79,

Papadopoulos, C. A. and Dimarogonas, A. D. , 1987, "Coupled Longitudinal and Bending Vibrations of a Rotating Shaft with an Open Crack", J of Sound and Vibration, 117(1), 81-93

Qian, G. L., Gu, S. N. and Jiang, J. S. , 1990, "The Dynamic Behavior and Crack Detection of a Beam With a Crack", J of Sound and Vibration, 138(2), pp 233-243

Sekhar, A. S. and Prabhu, B. S. , 1992, "Crack Detection and Vibration Characteristics of Cracked Shafts", J. of Sound and Vibration, 157(2), pp 375-381

Tada, H., Paris, P. and Irwin,G. , 1973, "The Stress Analysis of Cracks Handbook", Del Research Corporation, Hellertown, Pennsylvania

Weaver, W., Jr. and Johnston, P. R. , 1987, "Structural Dynamics by Finite Elements", Prentice-Hall,INC., Englewood Cliffs,New Jersey

Westergaard, H. M. , 1939, "Bearing Pressures and Cracks", Transactions, ASME, Journal of Applied Mechanics, Series A, Vol. 66, pp 49.

Ziebarth, H. and Baumgartner, R. J. , 1981, Early Detection of Cross-sectional Rotor Cracks by Turbine Shaft Vibration Monitoring Techniques", ASME-paper 81-JPGC-Pwr-26

Appendices

Appendix A

Free Vibration of a Beam

A.1 Bending Vibration Equation of a Beam Subjected to an Axial Force

For a beam with different boundary conditions, the derivation of the vibration equation is given below.

Consider the free body diagram of an element of a beam shown in Figure A.1 where M(x,t) is the bending moment, V(x,t) is the shear force, and f(x,t) is the external force per unit length of the beam.

Since the inertia force acting on the element of the beam is

$$\rho A(x)dx\frac{\partial^2 w}{\partial t^2}(x,t) \tag{A.1}$$

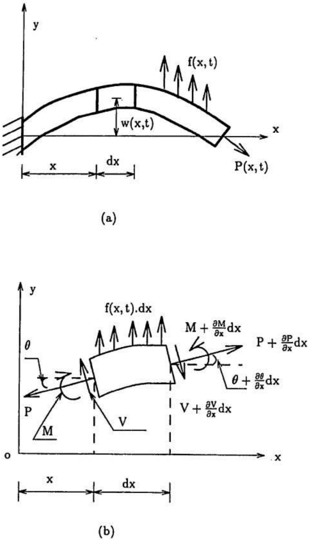

Figure A.1: (a) a beam in bending; (b) free body diagram of an element

Then the force equation of motion in the y direction gives

$$-(V+\frac{\partial V}{\partial x}dx)+fdx+V+(P+dP)Sin(\theta+d\theta)-PSin\theta=\rho Adx\frac{\partial^2 w}{\partial t^2} \quad (A.2)$$

Where ρ is the mass density, A(x) is the cross-sectional area of the beam and θ is the angle between the force P and the x-axis. The moment equation of motion about a point o is, (neglecting rotary inertia)

$$(M+dM)-(V+dV)dx+fdx\frac{dx}{2}-M=0 \quad (A.3)$$

By writing

$$dV=\frac{\partial V}{\partial x}dx \ and \ dM=\frac{\partial M}{\partial x}dx$$

and neglecting higher order terms. Equations (A.2) and (A.3) can be written as

$$-\frac{\partial V(x,t)}{\partial x}dx+fdx+(P+dP)Sin(\theta+d\theta)-PSin\theta=\rho A(x,t)\frac{\partial^2 w}{\partial t^2}dx \quad (A.4)$$

$$\frac{\partial M(x,t)}{\partial x}-V(x,t)=0 \quad (A.5)$$

For small deflection

$$Sin(\theta+d\theta)\approx\theta+d\theta=\theta \quad (A.6)$$

From the elementary theory of bending of beams , the relationship between bending moment and deflection can be expressed as

$$M(x,t)=EI(x)\frac{\partial^2 w(x,t)}{\partial x^2} \quad (A.7)$$

Where E is Young's modulus and I(x) is the moment of inertia of the beam cross sectional area about the neutral axis. Substituting equation (A.7) into equation (A.4) and (A.5), we obtain the differential equation of motion for the forced lateral vibration of a nonuniform beam.

$$\frac{\partial^2}{\partial x^2}[EI(x)\frac{\partial^2 w(x,t)}{\partial x^2}]+\rho A(x)\frac{\partial^2 w(x,t)}{\partial t^2}-P\frac{\partial^2 w(x,t)}{\partial x^2}=f(x,t) \quad (A.8)$$

For the free vibration of a uniform beam, equation (A.8) reduces to

$$EI\frac{\partial^4 w(x,t)}{\partial x^4} + \rho A\frac{\partial^2 w(x,t)}{\partial t^2} - P\frac{\partial^2 w(x,t)}{\partial x^2} = 0 \tag{A.9}$$

Appendix B

Mass and Stiffness Matrices Derivation of Space Beam Element

Figure B.1(a) depicts a typical member i of a space frame. Each end of the member has six degrees of freedoms, three translation degrees and three rotational degrees. The principal planes of bending are the $x' - y'$ plane and $x' - z'$ plane. Six numbered displacements indicated at each end of the member, consist of translations and rotations in the x', y', z' direction. With a prismatic member, the 12×12 stiffness matrix for local axes is composed of the following 6×6 submatrices. (Weaver and Johnston, 1987).

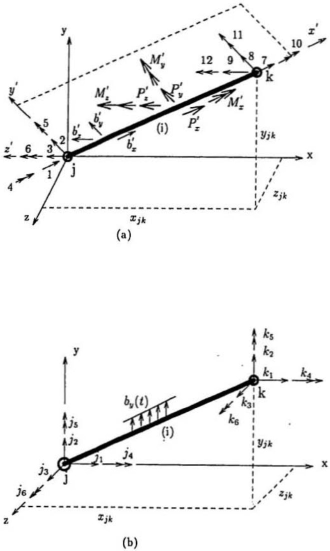

Figure B.1: Space frame member: (a) local directions; (b) global directions.

$$[K'_{jj}] = \frac{E}{L^3}\begin{bmatrix} r_1 I_z & 0 & 0 & 0 & 0 & 0 \\ 0 & 12I_z & 0 & 0 & 0 & 6LI_z \\ 0 & 0 & 12I_y & 0 & -6LI_y & 0 \\ 0 & 0 & 0 & r_2L^2I_y & 0 & 0 \\ 0 & 0 & -6LI_y & 0 & 4L^2I_y & 0 \\ 0 & 6LI_z & 0 & 0 & 0 & 4L^2I_z \end{bmatrix} \quad \text{(B.1)}$$

$$[K'_{kj}] = \frac{E}{L^3}\begin{bmatrix} -r_1 I_z & 0 & 0 & 0 & 0 & 0 \\ 0 & -12I_z & 0 & 0 & 0 & -6LI_z \\ 0 & 0 & -12I_y & 0 & 6LI_y & 0 \\ 0 & 0 & 0 & -r_2L^2I_y & 0 & 0 \\ 0 & 0 & -6LI_y & 0 & 2L^2I_y & 0 \\ 0 & 6LI_z & 0 & 0 & 0 & 2L^2I_z \end{bmatrix} \quad \text{(B.2)}$$

$$[K'_{kk}] = \frac{E}{L^3}\begin{bmatrix} r_1 I_z & 0 & 0 & 0 & 0 & 0 \\ 0 & 12I_z & 0 & 0 & 0 & -6LI_z \\ 0 & 0 & 12I_y & 0 & 6LI_y & 0 \\ 0 & 0 & 0 & r_2L^2I_y & 0 & 0 \\ 0 & 0 & 6LI_y & 0 & 4L^2I_y & 0 \\ 0 & -6LI_z & 0 & 0 & 0 & 4L^2I_z \end{bmatrix} \quad \text{(B.3)}$$

Where ρ is the mass density of element, A is the area of the cross section of beam, L is the length of element,I_x is the polar moment of inertia of the cross section, I_y I_z are its second moments of area about the y' and z' axis respectively. r_2 is GI_x/EI_y, r_1 is AL^2/I_z.

For the circular cross section

$$I_x = \frac{\pi D^4}{32}$$

$$I_y = \frac{\pi D^4}{64}$$

$$I_z = \frac{\pi D^4}{64}$$

D is the diameter of the shaft
G is the shear modulus of elasticity

$$G = \frac{E}{2(1+\nu)}$$

The stiffness matrix of element is

$$[K'] = \begin{bmatrix} K'_{jj} & K'_{jk} \\ K'_{kj} & K'_{kk} \end{bmatrix} \tag{B.4}$$

Similarly, the 12× 12 consistent - mass matrix M' for local directions contains the four 6 × 6 submatrices,

$$[M'_{jj}] = \frac{\rho AL}{420} \begin{bmatrix} 140 & 0 & 0 & 0 & 0 & 0 \\ 0 & 156 & 0 & 0 & 0 & 22L \\ 0 & 0 & 156 & 0 & -22L & 0 \\ 0 & 0 & 0 & 140r_g^2 & 0 & 0 \\ 0 & 0 & -22L & 0 & 4L^2 & 0 \\ 0 & 22L & 0 & 0 & 0 & 4L^2 \end{bmatrix} \tag{B.5}$$

$$[M'_{kj}] = \frac{\rho AL}{420} \begin{bmatrix} 70 & 0 & 0 & 0 & 0 & 0 \\ 0 & 54 & 0 & 0 & 0 & 13L \\ 0 & 0 & 54 & 0 & -13L & 0 \\ 0 & 0 & 0 & 70r_g^2 & 0 & 0 \\ 0 & 0 & 13L & 0 & -3L^2 & 0 \\ 0 & -13L & 0 & 0 & 0 & -3L^2 \end{bmatrix} \tag{B.6}$$

$$[M'_{kk}] = \frac{\rho AL}{420} \begin{bmatrix} 140 & 0 & 0 & 0 & 0 & 0 \\ 0 & 156 & 0 & 0 & 0 & -22L \\ 0 & 0 & 156 & 0 & 22L & 0 \\ 0 & 0 & 0 & 140r_g^2 & 0 & 0 \\ 0 & 0 & 22L & 0 & 4L^2 & 0 \\ 0 & -22L & 0 & 0 & 0 & 4L^2 \end{bmatrix} \tag{B.7}$$

Where r_g^2 is J/A , the radius of gyration squared, J is the mass polar moment of inertia of shaft per unit length.

$$J = \frac{\pi D^4}{32}$$

The Consistent - mass matrix M' is

$$[M'] = \begin{bmatrix} M'_{jj} & M'_{jk} \\ M'_{kj} & M'_{kk} \end{bmatrix} \tag{B.8}$$

For the lateral(transverse) vibration of a shaft, it is reasonable to neglect the translation and rotation in the axial direction. Therefore the stiffness matrix and consistent - mass matrix of an element can be expressed as follows:

$$[K'_{jj}] = \frac{E}{L^3}\begin{bmatrix} 12I_z & 0 & 0 & 6LI_z \\ 0 & 12I_y & -6LI_y & 0 \\ 0 & -6LI_y & 4L^2I_y & 0 \\ 6LI_z & 0 & 0 & 4L^2I_z \end{bmatrix} \tag{B.9}$$

$$[K'_{kj}] = \frac{E}{L^3}\begin{bmatrix} -12I_z & 0 & 0 & -6LI_z \\ 0 & -12I_y & 6LI_y & 0 \\ 0 & -6LI_y & 2L^2I_y & 0 \\ 6LI_z & 0 & 0 & 2L^2I_z \end{bmatrix} \tag{B.10}$$

$$[K'_{kk}] = \frac{E}{L^3}\begin{bmatrix} 12I_z & 0 & 0 & -6LI_z \\ 0 & 12I_y & 6LI_y & 0 \\ 0 & 6LI_y & 4L^2I_y & 0 \\ -6LI_z & 0 & 0 & 4L^2I_z \end{bmatrix} \tag{B.11}$$

The stiffness matrix of element K' is

$$[K'] = \begin{bmatrix} K'_{jj} & K'_{jk} \\ K'_{kj} & K'_{kk} \end{bmatrix} \tag{B.12}$$

Figure B.2 depicts an element neglecting the translation and rotation in the axial direction.

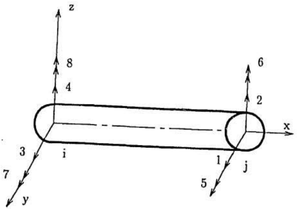

Figure B.2: Beam element with 8 degrees of freedom

Similarly, the 8×8 consistent - mass matrix M' for local directions contains the four 4×4 submatrices,

$$[M'_{jj}] = \frac{\rho AL}{420}\begin{bmatrix} 156 & 0 & 0 & 22L \\ 0 & 156 & -22L & 0 \\ 0 & -22L & 4L^2 & 0 \\ 22L & 0 & 0 & 4L^2 \end{bmatrix} \tag{B.13}$$

$$[M'_{kj}] = \frac{\rho AL}{420}\begin{bmatrix} 54 & 0 & 0 & 13L \\ 0 & 54 & -13L & 0 \\ 0 & 13L & -3L^2 & 0 \\ -13L & 0 & 0 & -3L^2 \end{bmatrix} \tag{B.14}$$

$$[M'_{kk}] = \frac{\rho AL}{420}\begin{bmatrix} 156 & 0 & 0 & -22L \\ 0 & 156 & 22L & 0 \\ 0 & 22L & 4L^2 & 0 \\ -22L & 0 & 0 & 4L^2 \end{bmatrix} \tag{B.15}$$

The Consistent - mass matrix M' is

$$[M'] = \begin{bmatrix} M'_{jj} & M'_{jk} \\ M'_{kj} & M'_{kk} \end{bmatrix} \tag{B.16}$$

After stiffness matrix, mass matrix for individual elements have been transformed to global directions, we can assemble them by direction stiffness method (Weaver and Johnston, 1987). Then the stiffness and mass matrices of the whole structure can be obtained.

After obtaining the K, M of whole structure, the matrix equation of free vibration can be written as follows:

$$[M]\{\ddot{q}\} + [K]\{q\} = \{0\} \tag{B.17}$$

Appendix C

Flow Chart of Program

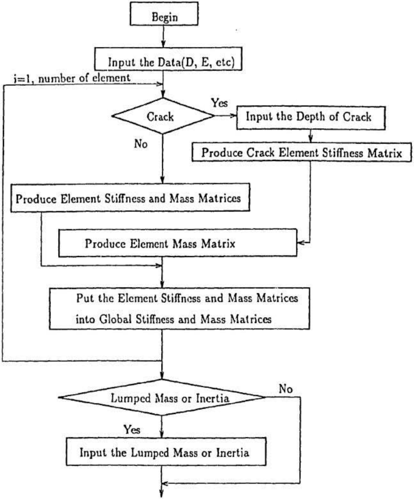
Begin
Input the Data(D, E, etc)
i=1, number of element
Crack
Yes
No
Input the Depth of Crack
Produce Crack Element Stiffness Matrix
Produce Element Stiffness and Mass Matrices
Produce Element Mass Matrix
Put the Element Stiffness and Mass Matrices
into Global Stiffness and Mass Matrices
Lumped Mass or Inertia
No
Yes
Input the Lumped Mass or Inertia

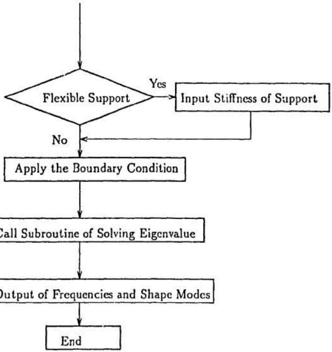
Flexible Support
Yes
Input Stiffness of Support
No
Apply the Boundary Condition
Call Subroutine of Solving Eigenvalue
Output of Frequencies and Shape Modes
End

Appendix D

Computer Program in Fortran-77

```
      DIMENSION  XM(120,120),XK(120,120),XNODE(30,2),MELM(30,4)
      DIMENSION   AIEU(5,4), XDCRACK(10),FLEC(4,4),XKCRACK(8,8)
      DIMENSION   T(8,4),TT(4,8),TWORK(8,4),XCO(4,4),FCRACK(4,4),
   C        FFCRACK(4,8),XKLOC(8,8),XMLOC(8,8),NBOU(50,3)
   C        ,H(120,120),V(120),ESPRING(20),XMODE(30),XLUMP(20),
   C        LUMP(20,2)

      CHARACTER*8 XCHAR
      OPEN(1,FILE='in.dat',STATUS='OLD')
      OPEN(2,FILE='out.dat',STATUS='NEW')
      OPEN(3,FILE='out1.dat',STATUS='NEW')
      OPEN(4,FILE='out2.dat',STATUS='NEW')
C     XM --- GLOBAL MASS MATRIX
C     XK --- GLOBAL STIFFNESS MATRIX
C     XNODE(*, 2) -- COORDINATE OF NODE, x
C     MELM(1,2,3,4) --ELEMENT
C                    1 -- START No.
C                    2 -- END   No.
C                    3 -- TYPE OF MATERIAL
C                    4 -- TYPE OF ELM.  0 -- UNCRACKED.
C                             1,2, ... -- CRACKED
C     AIEU(1,2,3,4,5,6) -- MATERIAL OF ELM.
C                    1 -- RADIUS OF CROSS=SECTION
C     X              2 -- INTERIA MOMENT AT X -DIR.
C     X              3 --       "          Y  "
C                    4 -- E, YOUNG MODULA
C                    5 -- POSSION'S RATIO
C                    6 -- MASS DENSITY
C     MELM -- No. OF ELEMENTS
C     XCRACK(1) - THE DEPTH OF CRACK
C                    1 - DEPTH
C             NCR -- THE NO. OF CRACK

      READ(1,*)NFE,NNODE,NELM,NETYPE,NBO,NKSPRING,NCR,NMASS

      READ(1,*)((XNODE(I,J),J=1,2),I=1,NNODE)
      READ(1,*)((MELM(I,J),J=1,4),I=1,NELM)
      READ(1,*)((AIEU(I,J),J=1,4),I=1,NETYPE)
      READ(1,*)((NBOU(I,J),J=1,3),I=1,NBO)
      IF(NKSPRING.GT.0)THEN
      READ(1,*)(ESPRING(I),I=1,NKSPRING)
      ELSE IF(NCR.GT.0)THEN

      READ(1,*)(XDCRACK(I),I=1,NCR)
      ELSE IF(NMASS.GT.0)THEN
      READ(1,*)(XLUMP(I),I=1,NMASS)
      READ(1,*)((LUMP(I,J),J=1,2),I=1,NMASS)
      ENDIF
```

```
C             NFE -- FREDOM OF EACH NODE
C             NNODE -- NO. OF NODES
C             NELM -- NO. OF ELM.
C             NETYPE --NO. OF ELMTYPE(MATERIAL)
C             NMASS - No. of LUMPED MASS(note: freedom)
C             LUMP(1,2)---
C                     1---No. of NODE
C                     2---No. of freedom(1,2)
C             XLUMP(20)---Mass or inerti

      NNFR=NNODE*NFE
C             NNFR -- NO. OF FREDOM OF STRUCTURE

C             NFE -- THE No. OF FREDOM IS 4
C             XLOU -- THE MASS DENSITY
C             NKSPRING -- NO. OF ELASTIC  SPRING  SUPPORTS
      NNFR=NNODE*4
      NNFE=2*NFE
      DO 1000 IELM=1,NELM
      KCRACK=MELM(IELM,4)
C                     THE No. OF THE CRACK
      KINDELM=MELM(IELM,3)
      NSTA=MELM(IELM,1)
      NEND=MELM(IELM,2)
      X1=XNODE(NSTA,1)
      X2=XNODE(NEND,1)
      Y1=XNODE(NSTA,2)
      Y2=XNODE(NEND,2)
      XLELM=SQRT((X2-X1)**2+(Y2-Y1)**2)

      PAI=3.1415926

      R=AIEU(KINDELM,1)
      XA=PAI*R**2
      XIZ=PAI*R**4/4.
      XIY=XIZ
C     XIZ=AIEU(KINDELM,2)
C     XIY=AIEU(KINDELM,3)
      E=AIEU(KINDELM,2)
      XNU=AIEU(KINDELM,3)
      XLOU=AIEU(KINDELM,4)
C     MASS MATRIX

      CALL XLOCM(XLELM,XLOU,XA,XMLOC,NNFE)
```

```
      WRITE(3,222)XLELM,XLOU,XA,NFE
222   FORMAT(1X,'L=',F5.2,'LOU=',F7.2,'A=',F10.4,'NF=',I2)
      WRITE(3,444)((XMLOC(I,J),J=1,8),I=1,8)
444   FORMAT(1X,'MLOC=',4F14.4)
      DO 777 II=1,NFE
      DO 777 JJ=1,NFE
      XM(NFE*(NSTA)-NFE+II,NFE*(NSTA)-NFE+JJ)=
     C        XM(NFE*(NSTA)-NFE+II,NFE*(NSTA)-NFE+JJ)+XMLOC(II,JJ)
      XM(NFE*(NSTA)-NFE+II,NFE*(NEND)-NFE+JJ)=
     C XM(NFE*(NSTA)-NFE+II,NFE*(NEND)-NFE+JJ)+XMLOC(II,JJ+NFE)
      XM(NFE*(NEND)-NFE+II,NFE*(NSTA)-NFE+JJ)=
     C XM(NFE*(NEND)-NFE+II,NFE*(NSTA)-NFE+JJ)+XMLOC(II+NFE,JJ)
      XM(NFE*(NEND)-NFE+II,NFE*(NEND)-NFE+JJ)=
     C XM(NFE*(NEND)-NFE+II,NFE*(NEND)-NFE+JJ)+XMLOC(II+NFE,JJ+NFE)
777   CONTINUE


      IF (KCRACK.EQ.0) THEN
      CALL XLOCK(E,XLELM,XIZ,XIY,XKLOC,NNFE)
      WRITE(3,555)KCRACK,E,XIZ,XIY
555   FORMAT(1X,'KCRACK=',I2,'E=',E14.4,'IZ AND IY',2F10.4)
      WRITE(3,333)((XKLOC(I,J),J=1,8),I=1,8)
333   FORMAT(1X,
     C        'KLOC=',4E16.4)


      ELSE
      CDEPTH=XDCRACK(KCRACK)
C             THE DEPTH OF KCRACK CRACK
C     XDCRACK(  ) -- CRACK DEPTH OF EACK CRACK
      PRINT *,'CDEPTH',CDEPTH,'R=',R
      CALL XCRACK(FLEC,XLELM,XKLOC,NFE,CDEPTH,R,E,XNU,XCO
     C        ,XIZ,FCRACK,FFCRACK,T,TT,TWORK)
c     SUB  XCRACK(FLEC,XL,XKCRACK,NFE,CDEPTH,R,E,XNU,XCO
c    C        ,XIZ,FCRACK,FFCRACK,T,TT,TWORK)
      WRITE(3,212)((XKLOC(I,J),J=1,8),I=1,8)
212   FORMAT(1X,
     C        'KLOCRACK=',4E16.4)

      END IF
      DO 666 II=1,NFE
      DO 666 JJ=1,NFE
      XK(NFE*(NSTA)-NFE+II,NFE*(NSTA)-NFE+JJ)=
     C        XK(NFE*(NSTA)-NFE+II,NFE*(NSTA)-NFE+JJ)+XKLOC(II,JJ)
      XK(NFE*(NSTA)-NFE+II,NFE*(NEND)-NFE+JJ)=
     C XK(NFE*(NSTA)-NFE+II,NFE*(NEND)-NFE+JJ)+XKLOC(II,JJ+NFE)
      XK(NFE*(NEND)-NFE+II,NFE*(NSTA)-NFE+JJ)=
     C XK(NFE*(NEND)-NFE+II,NFE*(NSTA)-NFE+JJ)+XKLOC(II+NFE,JJ)
      XK(NFE*(NEND)-NFE+II,NFE*(NEND)-NFE+JJ)=
     C XK(NFE*(NEND)-NFE+II,NFE*(NEND)-NFE+JJ)+XKLOC(II+NFE,JJ+NFE)
```

```
C       XK(NFE*(NSTA)-NFE+II,NFE*(NSTA)-NFE+JJ)=XKLOC(II,JJ)
C       XK(NFE*(NSTA)-NFE+II,NFE*(NEND)-NFE+JJ)=XKLOC(II,JJ)
C       XK(NFE*(NEND)-NFE+II,NFE*(NSTA)-NFE+JJ)=XKLOC(II,JJ)
C       XK(NFE*(NEND)-NFE+II,NFE*(NEND)-NFE+JJ)=XKLOC(II,JJ)
 666    CONTINUE
 1000   CONTINUE
        WRITE(3,305)((XK(I,J),J=1,NNFR),I=1,NNFR)
 305    FORMAT(1X,'K=',4E16.4)
        WRITE(3,306)((XM(I,J),J=1,NNFR),I=1,NNFR)
 306    FORMAT(1X,'M=',4E16.4)

        WRITE(3,404)(XM(I,I),I=1,NNFR)
 404    FORMAT(1X,'MII=',4E16.4)
        WRITE(3,403)(XK(I,I),I=1,NNFR)
 403    FORMAT(1X,'KII=',4E16.4)


C       Intruduce Lumped Mass and Inertia

        IF(NMASS.GT.0) THEN
        DO 767 I=1,NMASS
        ILN=LUMP(I,1)
        ILF=LUMP(I,2)
        XMLU=XLUMP(I)
        III=(ILN-1)*4+ILF
        print *,'Nmass',nmass,'ILN',ILN,'ILF',ILF,'XMLU',
     c  XMLU,'III',III
        XM(III,III)=XM(III,III)+XMLU
        print *,'XM(III,III)',XM(III,III)
 767    CONTINUE
        ELSE
        ENDIF

C       end of intrucing lumped Mass and Inertia
c       INTRODUCE THE BOUNDARY CODITIONS

C       NBOU(1,2,3)
C               1 -- NO. OF NODE
C               2 -- FRODOM OF RESTRAINED NODE
C               3 -- TYPE OF RESTRAIN  0 -- RIGID,
c                                 1 2,3 ..-- ELASTIC
c                                 1 -- K1, 2 -- K2, ...
c       NBO -- THE NO. OF RESTRAINED NODE(* REPEATED NODE)
c       NKSPRING -- NO. OF ELASTIC SUPPORTS
C       ESPRING(NKSPRING) -- STIFFNESS OF SPRING

        DO 888 I=1,NBO
        NB1=NBOU(I,1)
        NB2=NBOU(I,2)
        NB3=NBOU(I,3)
        IB1=4*(NB1-1)+NB2
        IF(NB3.EQ.0) THEN
```

```
            DO 999 IB=1,NNFR
            XK(IB1,IB)=0.
            XK(IB,IB1)=0.
 999        CONTINUE
      XK(IB1,IB1)=999999999999999.
            DO 678 IB=1,NNFR
            XM(IB1,IB)=0.
            XM(IB,IB1)=0.
 678        CONTINUE
      XM(IB1,IB1)=2*999999999999999.

      ELSE
      ESPR=ESPRING(NB3)
      XK(IB1,IB1)=XK(IB1,IB1)+ESPR

      END IF
 888  CONTINUE
      PRINT *,'EIGEN'
      WRITE(3,303)((XK(I,J),J=1,NNFR),I=1,NNFR)
 303  FORMAT(1X,'KB=',4E16.4)
      WRITE(3,304)((XM(I,J),J=1,NNFR),I=1,NNFR)
 304  FORMAT(1X,'MB=',4E16.4)

      WRITE(3,504)(XM(I,I),I=1,NNFR)
 504  FORMAT(1X,'MII=',4E16.4)
      WRITE(3,503)(XK(I,I),I=1,NNFR)
 503  FORMAT(1X,'KII=',4E16.4)

      PRINT *,'NNFR=',NNFR
      ERR=0.000001
      CALL EIGG(XK,XM,H,V,ERR,NNFR,120)

C     ERR -- ACCURACY OF ITERATION
C     NMODE -- NO. OF MODE
C     H -- EIGENVECTOR

      WRITE(2,1002)(XK(I,I),I=1,NNFR)
 1002 FORMAT(1X,'EIGENVALUE'/1X,4E16.9)

      DO 343 II=NNFR,1,-1

      DO 345 I=1,NFE
      DO 346 IN=1,NNODE
      IM1=NFE*(IN-1)+I
      XMODE(IN)=XM(IM1,II)
 346  CONTINUE
      IF(I.EQ.1)THEN
      XCHAR='Z-MODE'
      ELSE IF(I.EQ.2) THEN
      XCHAR='Y-MODE'
      ELSE IF(I.EQ.3) THEN
```

```
      XCHAR='CTZ-MODE'
      ELSE IF(I.EQ.4) THEN
      XCHAR='CTY-MODE'
      END IF
      WRITE(2,989)II,XCHAR
 989  FORMAT(1X,'MODE NO.',I3,3X,A8)
      WRITE(2,988)(XMODE(IMM),IMM=1,NNODE)
 988  FORMAT(1X,5E14.6)
 345  CONTINUE
 343  CONTINUE


      WRITE(2,1001)((XM(I,J),J=1,NNFR),I=1,NNFR)
 1001 FORMAT(1X,'EIGENVECTOR'/1X,4E16.9)
      STOP
      END

      SUBROUTINE MCFL(CDEPTH,R,FLEC,E,XNU,NC)
C     NC--the num. of fredom of crack flexibility matrix
c         NC=4 ---- neglect torsional  and longitunal vib.
c         NC=6 ---- include      "
c     R--- Radis of shaft
c     CDEPTH -- depth of crack
c     E -- young module
c     xnu -- Possion's ratio
C     FELC -- flexibility matrix of crack elm.
      DIMENSION FLEC(NC,NC)
      CRATIO=CDEPTH/2./R
      DO 10 I=1,NC
      FLEC(I,J)=0 0
 10   CONTINUE
      IF(NC.EQ.6) THEN
      PRINT *, 'NC=',NC,'WRONG FREDOM OF CRACK'
      STOP
      END IF
      CALL C22(CRATIO,FC22)
      CALL C33(CRATIO,FC33)
      CALL C44(CRATIO,FC44)
      CALL C45(CRATIO,FC45)
      CALL C55(CRATIO,FC55)
      print *,'22n=',fc22,'33=',fc33,'44=',fc44,
     c '55=',fc55,'54=',fc45

      FC22=10**FC22
      FC33=10**FC33
      FC44=10**FC44
      FC45=10**FC45
      FC55=10**FC55
      print *,'22=',fc22,'33=',fc33,'44=',fc44,
     c '55=',fc55,'54=',fc45
```

```
      FC22=10**FC22
      FC33=10**FC33
      FC44=10**FC44
      FC45=10**FC45
      FC55=10**FC55
      print *,'22=',fc22,'33=',fc33,'44=',fc44,
     c '55=',fc55,'54=',fc45

      PAI=3.1415926
      F0=PAI*E*R**2/(1.-XNU**2)
      FLEC(1,1)=FC22*R/F0
      FLEC(2,2)=FC33*R/F0
      FLEC(3,3)=FC44/R/F0
      FLEC(4,4)=FC55/R/F0
      FLEC(4,3)=FC45/R/F0
      FLEC(3,4)=FLEC(4,3)
      PRINT *, 'CRATIO=',CRATIO, 'FC=',((FLEC(I,J),
    c J=1,NC),I=1,NC)
      RETURN
      END


      SUBROUTINE XCRACK(FLEC,XL,XKLOC,NFE,CDEPTH,R,E,XNU,XC0
     C          ,XIZ,FCRACK,FFCRACK,T,TT,TWORK)
      DIMENSION FLEC(4,4),XKLOC(8,8),T(8,4),TT(4,8),TWORK(8,4),
     C          XC0(4,4),FCRACK(4,4),FFCRACK(4,8)
      DO 10 I=1,8
      DO 10 J=1,4
      T(I,J)=0.
      TT(J,I)=0.
10    CONTINUE
      DO 20 I=1,8
      DO 20 J=1,8
      XKLOC(I,J)=0.0
20    CONTINUE
      CALL MCFL(CDEPTH,R,FLEC,E,XNU,NFE)
      DO 30 I=1,4
      T(I,I)=-1.
      T(I+4,I)=1.
30    CONTINUE
      T(3,2)=XL
      T(4,1)=-XL
      print *,'T[]=',((T(I,J),J=1,NFE),I=1,8)
      CALL XK22(XL,XC0,E,XIZ,NFE)
      print *,'XC0[]=',((XC0(I,J),J=1,NFE),I=1,NFE)

      DO 40 I=1,NFE
      DO 40 J=1,NFE
      FCRACK(I,J)=FLEC(I,J)+XC0(I,J)
40    CONTINUE
      NNFE=2*NFE
```

```
      print *,'FCRACK[]=',((FCRACK(I,J),J=1,NFE),I=1,NFE)
      DO 41 I=1,NFE
      DO 41 J=1,NFE
      FCRACK(I,J)=FCRACK(I,J)*E
 41   CONTINUE
      print *,'FCRACK[]=',((FCRACK(I,J),J=1,NFE),I=1,NFE)

      CALL INVER(NFE,FFCRACK,FCRACK,NNFE)
       PRINT *,'INVER'
      print *,'FCRACKINV[]=',((FCRACK(I,J),J=1,NFE),I=1,NFE)

      DO 42 I=1,NFE
      DO 42 J=1,NFE
      FCRACK(I,J)=FCRACK(I,J)*E
 42   CONTINUE
      PRINT *,'FCRACK',((FCRACK(I,J),J=1,NFE),I=1,NFE)
C     FFCRACK(NFE,2NFE)

      CALL TRAN(T,TT,8,4)
       PRINT *,'TRAN'

      CALL MTM(T,FCRACK,TWORK,8,4,4)
       PRINT *,'MTM1'

      CALL MTM(TWORK,TT,XKLOC,8,4,8)
       PRINT *,'MTM2'
      PRINT *,'TWORK',((TWORK(I,J),J=1,4),I=1,8)

      WRITE(4,102)((XKLOC(I,J),J=1,8),I=1,8)
 102  FORMAT(1X,'KCRACK',4E19.9)
      WRITE(*,102)((XKLOC(I,J),J=1,8),I=1,8)

      RETURN
      END

      SUBROUTINE XK22(XL,XC0,E,XIZ,NFE)
C     The program is used to calculated the flexibility of an
C                      uncracked elm.
      DIMENSION XC0(NFE,NFE)
      DO 10 I=1,NFE
      DO 10 J=1,NFE
      XC0(I,J)=0.
 10   CONTINUE
      XC0(1,1)=XL**3/3./E/XIZ
      XC0(2,2)=XL**3/3./E/XIZ
      XC0(3,3)=XL/E/XIZ
      XC0(4,4)=XL/E/XIZ
      XC0(3,2)=-XL**2/2./E/XIZ
      XC0(4,1)=XL**2/2./E/XIZ
      DO 20 I=1,NFE
      DO 20 J=I+1,NFE
```

```
      XCO(I,J)=XCO(J,I)
 20   CONTINUE
      WRITE(4,101)((XCO(I,J),J=1,NFE),I=1,NFE)
 101  FORMAT(1X,'XCO',4E15.5)
      RETURN
      END


      SUBROUTINE XLOCK(E,XL,XIZ,XIY,XKLOC,NNFE)
      DIMENSION XKLOC(NNFE,NNFE)
C     E -- YOUNG MO.
C     XL -- LENGTH OF ELEMENT
C     XIZ -- SECTION INTERIA MOMENT AT Z DIRECTION
C     XIY --                "           Y   "
C     XKLOC ---LOCAL STIFFNESS MATRIX OF ELEMENT, (NFE,NFE)
C     NFE --- No. OF FREDOM OF NODE
C                       NFE=4-- NEGLECT TORSIONAL AND LONGITUDAL
C                       NFE=6   INCLUDE         "
C     NNFE -- 2*NFE
      DO 10 I=1,NNFE
      DO 10 J=1,NNFE
      XKLOC(I,J)=0.0
 10   CONTINUE
      COEE=E/XL**3
      XKLOC(1,1)=12.*XIZ*COEE
      XKLOC(2,2)=12.*XIY*COEE
      XKLOC(3,3)=4.  *XL**2*XIY*COEE
      XKLOC(4,4)=4.  *XL**2*XIZ*COEE
      XKLOC(3,2)=-6.*XL*XIY*COEE
      XKLOC(4,1)=6.  *XL*XIZ*COEE
      XKLOC(2,3)=XKLOC(3,2)
      XKLOC(1,4)=XKLOC(4,1)

      XKLOC(5,1)=-12.*XIZ*COEE
      XKLOC(5,4)=-6.*XL*XIZ*COEE
      XKLOC(6,2)=-12.*XIY*COEE
      XKLOC(6,3)=6.*XL*XIY*COEE
      XKLOC(7,2)=-6.*XL*XIY*COEE
      XKLOC(7,3)=2.*XL**2*XIY*COEE
      XKLOC(8,1)=6.*XL*XIZ*COEE
      XKLOC(8,4)=2.*XL**2*XIZ*COEE

      XKLOC(5,5)=12.*XIZ*COEE
      XKLOC(6,6)=12.*XIY*COEE
      XKLOC(7,7)=4.  *XL**2*XIY*COEE
      XKLOC(8,8)=4.  *XL**2*XIZ*COEE
      XKLOC(7,6)=6.*XL*XIY*COEE
      XKLOC(8,5)=-6.  *XL*XIZ*COEE
```

```
      DO 20 I=1,NNFE
      DO 20 J=I+1,NNFE
      XKLOC(I,J)=XKLOC(J,I)
 20   CONTINUE
      RETURN
      END

      SUBROUTINE XLOCM(XL,XLOU,XA,XMLOC,NNFE)
      DIMENSION XMLOC(NNFE,NNFE)
C     E -- YOUNG MO.
C     XLOU -- MASS DENSITY
C     XA -- AREA OF CROSS SECTION OF SHAFT
C     XL -- LENGTH OF ELEMENT
C     XIZ -- SECTION INTERIA MOMENT AT Z DIRECTION
C     XIY --              "                 Y     "
C     XKLOC ---LOCAL MASS MATRIX OF ELEMENT, (NFE,NFE)
C     NFE --- No. OF FREDOM OF NODE
C                    NFE=4-- NEGLECT TORSIONAL AND LONGITUDAL
C                    NFE=6   INCLUDE               "
      DO 10 I=1,NNFE
      DO 10 J=1,NNFE
      XMLOC(I,J)=0.0
 10   CONTINUE
      COEE=XLOU*XA*XL/420.
      XMLOC(1,1)=156.*COEE
      XMLOC(2,2)=156.*COEE
      XMLOC(3,3)=4. *XL**2*COEE
      XMLOC(4,4)=4. *XL**2*COEE
      XMLOC(3,2)=-22.*XL*COEE
      XMLOC(4,1)=22.*XL*COEE
      XMLOC(2,3)=XMLOC(2,3)
      XMLOC(1,4)=XMLOC(4,1)

      XMLOC(5,1)=54.*COEE
      XMLOC(5,4)=13.*XL*COEE
      XMLOC(6,2)=54.*COEE
      XMLOC(6,3)=-13.*XL*COEE
      XMLOC(7,2)=13.*XL*COEE
      XMLOC(7,3)=-3.*XL**2*COEE
      XMLOC(8,1)=-13.*XL*COEE
      XMLOC(8,4)=-3.*XL**2*COEE

      XMLOC(5,5)=156.*COEE
      XMLOC(6,6)=156.*COEE
      XMLOC(7,7)=4. *XL**2*COEE
      XMLOC(8,8)=4. *XL**2*COEE
      XMLOC(7,6)=22.*XL*COEE
      XMLOC(8,5)=-22. *XL*COEE
```

```
      DO 20 I=1,NNFE
      DO 20 J=I+1,NNFE
      XMLOC(I,J)=XMLOC(J,I)
 20   CONTINUE
      RETURN
      END




      SUBROUTINE LINE(X1,Y1,X2,Y2,X,Y)
      Y=Y1+(X-X1)*(Y2-Y1)/(X2-X1)
      RETURN
      END


      SUBROUTINE COFI(A0,A1,A2,A3,A4,A5,A6,A7,A8,A9,A10
     C        ,B0,B1,B2,B3,B4,B5,B6,B7,B8,B9,B10,A,B)
C     PRINT *,'A=',A,'B=',B
      IF(A.LT.A0) THEN
      PRINT *,'THE DEPTH OF CRACK IS WRONG'
        ELSE    IF((A.GE.A0).AND.(A.LE.A1)) THEN
          CALL LINE(A0,B0,A1,B1,A,B)
        ELSE    IF((A.GE.A1).AND.(A.LE.A2)) THEN
          CALL LINE(A1,B1,A2,B2,A,B)
          ELSE    IF((A.GE.A2).AND.(A.LE.A3)) THEN
             CALL LINE(A2,B2,A3,B3,A,B)
             ELSE       IF((A.GE.A3).AND.(A.LE.A4)) THEN
                  CALL LINE(A3,B3,A4,B4,A,B)
                  ELSE    IF((A.GE.A4).AND.(A.LE.A5)) THEN
                    CALL LINE(A4,B4,A5,B5,A,B)
                    ELSE    IF((A.GE.A5).AND.(A.LE.A6)) THEN
                      CALL LINE(A5,B5,A6,B6,A,B)
                      ELSE     IF((A.GE.A6).AND.(A.LE.A7)) THEN
                         CALL LINE(A6,B6,A7,B7,A,B)
                         ELSE     IF((A.GE.A7).AND.(A.LE.A8)) THEN
              CALL LINE(A7,B7,A8,B8,A,B)
              ELSE    IF((A.GE.A8).AND.(A.LE.A9)) THEN
          CALL LINE(A8,B8,A9,B9,A,B)
          ELSE    IF((A.GE.A9).AND.(A.LE.A10)) THEN
      CALL LINE(A9,B9,A10,B10,A,B)
                                            ELSE
C     IF(A.GT.A10) THEN
                                    PRINT *,'THE CRACK DEPTH IS WRONG'
      END IF
      RETURN
      END
```

```
      SUBROUTINE C22(CRATIO,FC22)
      A0=0.
      A1=0.1
      A2=0.2
      A3=0.3
      A4=0.4
      A5=0.5
      A6=0.6
      A7=0.7
      A8=0.8
      A9=0.9
      A10=1.0
      B0=-6.0
      B1=-1.7
      B2=-1.
      B3=-0.45
      B4=-0.13
      B5=0.1
      B6=0.3
      B7=0.5
      B8=0.85
      B9=1.3
      B10=1.85
      CALL COFI(A0,A1,A2,A3,A4,A5,A6,A7,A8,A9,A10,
C             B0,B1,B2,B3,B4,B5,B6,B7,B8,B9,B10,CRATIO,FC22)
      RETURN
      END

      SUBROUTINE C33(CRATIO,FC33)
      A0=0.
      A1=0.1
      A2=0.2
      A3=0.3
      A4=0.4
      A5=0.5
      A6=0.6
      A7=0.7
      A8=0.8
      A9=0.9
      A10=1.0
      B0=-6.
      B1=-1.7
      B2=-0.85
      B3=0.4
      B4=0.
      B5=0.2
      B6=0.4
      B7=0.65
      B8=1.0
      B9=1.5
      B10=2.28
```

```
      CALL COFI(A0,A1,A2,A3,A4,A5,A6,A7,A8,A9,A10,
C              B0,B1,B2,B3,B4,B5,B6,B7,B8,B9,B10,CRATIO,FC33)
      RETURN
      END


      SUBROUTINE C44(CRATIO,FC44)
      A0=0.
      A1=0.1
      A2=0.2
      A3=0.3
      A4=0.4
      A5=0.5
      A6=0.6
      A7=0.7
      A8=0.8
      A9=0.9
      A10=1.0
      B0=-6.
      B1=-1.82
      B2=-0.75
      B3=-0.085
      B4=0.4
      B5=1.0
      B6=1.5
      B7=2.
      B8=2.2
      B9=3.0
      B10=4.
      CALL COFI(A0,A1,A2,A3,A4,A5,A6,A7,A8,A9,A10,
C              B0,B1,B2,B3,B4,B5,B6,B7,B8,B9,B10,CRATIO,FC44)
      RETURN
      END


      SUBROUTINE C45(CRATIO,FC45)
      A0=0.
      A1=0.1
      A2=0.2
      A3=0.3
      A4=0.4
      A5=0.5
      A6=0.6
      A7=0.7
      A8=0.8
      A9=0.9
      A10=1.0
      B0=-6.
```

```
      B1=-1.18
      B2=-0.22
      B3=0.35
      B4=0.8
      B5=1.3
      B6=1.7
      B7=2.05
      B8=2.6
      B9=3.4
      B10=4.8
      CALL COFI(A0,A1,A2,A3,A4,A5,A6,A7,A8,A9,A10,
C             B0,B1,B2,B3,B4,B5,B6,B7,B8,B9,B10,CRATIO,FC45)
      RETURN
      END

      SUBROUTINE C55(CRATIO,FC55)
      A0=0.
      A1=0.1
      A2=0.2
      A3=0.3
      A4=0.4
      A5=0.5
      A6=0.6
      A7=0.7
      A8=0.8
      A9=0.9
      A10=1.0
      B0=-6.
      B1=-0.5
      B2=0.48
      B3=0.9
      B4=1.21
      B5=1.55
      B6=1.83
      B7=2.2
      B8=2.75
      B9=3.
      B10=3.
      CALL COFI(A0,A1,A2,A3,A4,A5,A6,A7,A8,A9,A10,
C             B0,B1,B2,B3,B4,B5,B6,B7,B8,B9,B10,CRATIO,FC55)
      RETURN
      END
```

```
      SUBROUTINE TRAN(T,TT,M,N)
      DIMENSION T(M,N),TT(N,M)
      DO 10 I=1,M
      DO 10 J=1,N
      TT(J,I)=T(I,J)
10    CONTINUE
      RETURN
      END

      SUBROUTINE MTM(A,B,C,M,N,L)
      DIMENSION A(M,N),B(N,L),C(M,L)
      DO 10 I=1,M
      DO 10 J=1,L
      C(I,J)=0.
      DO 20 K=1,N
      C(I,J)=C(I,J)+A(I,K)*B(K,J)
20    CONTINUE
10    CONTINUE
      RETURN
      END


      SUBROUTINE INVER(N,A,B,LL)
C     LL=2*N
      DIMENSION A(N,LL),B(N,N)
      INTEGER PV
      print *,'a',((a(i,j),j=1,ll),i=1,n)
      print *,'b',((b(i,j),j=1,n),i=1,n)
      DO 40 I=1,N
      DO 40 J=1,LL
      A(I,J)=0.0
40    CONTINUE
      DO 20 I=1,N
      DO 20 J=1,N
      A(I,J)=B(I,J)
20    CONTINUE
      DO 30 I=1,N
      J=I+N
      A(I,J)=1.
30    CONTINUE
      EPS=1.
10    IF(1.0+EPS.GT.1.0) THEN
      EPS=EPS/2.0
      GO TO 10
      END IF
      EPS=EPS*2
      PRINT *,'MACHIN EPSILON=',EPS
```

```
      EPS2=EPS*2
      DET=1.0
      DO 1010 I=1,N-1
      PV=I
        DO J=I+1,N
          IF(ABS(A(PV,I)).LT.ABS(A(J,I))) PV=J
        END DO
        IF(PV.NE.I)THEN
          DO JC=1,N*2
               TM=A(I,JC)
               A(I,JC)=A(PV,JC)
               A(PV,JC)=TM
          END DO
          DET=-DET
        END IF
        IF(A(I,I).EQ.0.) GO TO 1200
C     ELIMINATING BELOW DIAGONAL
        DO JR=I+1,N
          IF(A(JR,I).NE.0.)THEN
               R=A(JR,I)/A(I,I)
               DO KC=I+1,N*2
                 TEMP=A(JR,KC)
                 A(JR,KC)=A(JR,KC)-R*A(I,KC)
                 IF(ABS(A(JR,KC)).LT.EPS2*TEMP) A(JR,KC)=0.0
               END DO
          END IF
        END DO
 1010 CONTINUE
      DO I=1,N
              DET=DET*A(I,I)
      END DO
      PRINT *
      PRINT *,'DETER7BMINANT=',DET
      PRINT *
C     BACKWARD SUBSTITUTION
      IF(A(N,N).EQ.0) GOTO 1200
      DO 1100 M=N+1,N*2
              A(N,M)=A(N,M)/A(N,N)
              DO NV=N-1,1,-1
                      VA=A(NV,M)
                      DO K=NV+1,N
                              VA=VA-A(NV,K)*A(K,M)
                      END DO
                      A(NV,M)=VA/A(NV,NV)
              END DO
 1100 CONTINUE
      DO 99 I=1,N
      DO 99 J=N+1,N*2
```

```
      B(I,J-N)=A(I,J)
 99   CONTINUE
      RETURN
1200  PRINT *,'MATRIX IS SINGULAR'
      END



      subroutine EIGG(A,B,H,V,ERR,N,NX)
c     DIET{[A]-LANBTA*[B]} = 0

      DIMENSION V(NX),A(NX,NX),B(NX,NX),H(NX,NX)
      CALL DECOG(B,N,NX)
      CALL INVCH(B,H,N,NX)
      CALL BTAB3(A,H,V,N,NX)
      CALL JACOB(A,B,ERR,N,NX)
      CALL MATMB(H,B,V,N,NX)
      RETURN
      END

      SUBROUTINE DECOG(A,N,NX)
      DIMENSION A(NX,NX)
      IF(A(1,1))1,1,3
  1   WRITE(*,2)
  2   FORMAT('ZERO OR NEGATIVE RADICAND')
      GO TO 200
  3   A(1,1)=SQRT(A(1,1))
      DO 10 J=2,N
 10   A(1,J)=A(1,J)/A(1,1)
      DO 40 I=2,N
      I1=I-1
      D=A(I,I)
      DO 20 L=1,I1
 20   D=D-A(L,I)*A(L,I)
      IF(A(I,I))11,11,21
 11   WRITE(*,2)
      stop
 21   A(I,I)=SQRT(D)
      I2=I+1
      DO 40 J=I2,N
      D=A(I,J)
      DO 30 L=1,I1
 30   D=D-A(L,I)*A(L,J)
      A(I,J)=D/A(I,I)
 40   continue
      DO 50 I=2,N
```

```
      I1=I-1
      DO 50 J=1,I1
   50 A(I,J)=0.
C
  200 RETURN
      END


      SUBROUTINE INVCH(S,A,N,NX)
      DIMENSION A(NX,NX),S(NX,NX)
      DO 10 I=1,N
   10 A(I,I)=1./S(I,I)
      N1=N-1
      DO 100 K=1,N1
      NK=N-K
      DO 100 I=1,NK
      J=I+K
      D=0.
      I1=I+1
      IK=I+K
      DO 20 L=I1,IK
   20 D=D+S(I,L)*A(L,J)
  100 A(I,J)=-D/S(I,I)
C
      RETURN
      END

      SUBROUTINE BTAB3(A,B,V,N,NX)
      DIMENSION A(NX,NX),V(NX),B(NX,NX)
      DO 10 I=1,N
      DO 5 J=1,N
      V(J)=0.
      DO 5 K=1,N
    5 V(J)=V(J)+A(I,K)*B(K,J)
      DO 10 J=1,N
   10 A(I,J)=V(J)
      DO 20 J=1,N
      DO 15 I=1,N
      V(I)=0.
      DO 15 K=1,N
   15 V(I)=V(I)+B(K,I)*A(K,J)
      DO 20 I=1,N
   20 A(I,J)=V(I)
C
      RETURN
      END
```

```
      SUBROUTINE JACOB(A,V,ERR,N,NX)
      DIMENSION A(NX,NX),V(NX,NX)
      ITM=500
      IT=0
      DO 10 I=1,N
      DO 10 J=1,N
      IF(I-J)3,1,3
    3 V(I,J)=0.
      GO TO 10
    1 V(I,J)=1.
   10 CONTINUE
   13 T=0.
      M=N-1
      DO 20 I=1,M
      J1=I+1
      DO 20 J=J1,N
      IF(ABS(A(I,J))-T)20,20,2
    2 T=ABS(A(I,J))
      IR=I
      IC=J
   20 CONTINUE
      IF(IT)5,4,5
    4 T1=T*ERR
    5 IF(T-T1)999,999,6
    6 PS=A(IR,IR)-A(IC,IC)
      TA=(-PS+SQRT(PS*PS+4*T*T))/(2*A(IR,IC))
      C=1./SQRT(1+TA*TA)
      S=C*TA
      DO 50 I=1,N
      P=V(I,IR)
      V(I,IR)=C*P+S*V(I,IC)
   50 V(I,IC)=C*V(I,IC)-S*P
      I=1
  100 IF(I-IR)7,200,7
    7 P=A(I,IR)
      A(I,IR)=C*P+S*A(I,IC)
      A(I,IC)=C*A(I,IC)-S*P
      I=I+1
      GO TO 100
  200 I=IR+1
  300 IF(I-IC)8,400,8
    8 P=A(IR,I)
      A(IR,I)=C*P+S*A(I,IC)
      A(I,IC)=C*A(I,IC)-S*P
      I=I+1
      GO TO 300
  400 I=IC+1
  500 IF(I-N)9,9,600
```

```
    9   P=A(IR,I)
        A(IR,I)=C*P+S*A(IC,I)
        A(IC,I)=C*A(IC,I)-S*P
        I=I+1
        GO TO 500
  600   P=A(IR,IR)
        A(IR,IR)=C*C*P+2.*C*S*A(IR,IC)+S*S*A(IC,IC)
        A(IC,IC)=C*C*A(IC,IC)+S*S*P-2.*C*S*A(IR,IC)
        A(IR,IC)=0.
        IT=IT+1
        IF(IT-ITM)13,13,999
C
  999   RETURN
        END


        SUBROUTINE MATMB(A,B,V,N,NX)
        DIMENSION A(NX,NX),B(NX,NX),V(NX)
        DO 20 J=1,N
        DO 16 I=1,N
        V(I)=0.
        DO 16 K=1,N
   16   V(I)=V(I)+A(I,K)*B(K,J)
        DO 20 I=1,N
   20   B(I,J)=V(I)
C
        RETURN
        END
```